

Development of Tantalum Phenoxy-Imine Compounds for Selective Ethylene Oligomerization

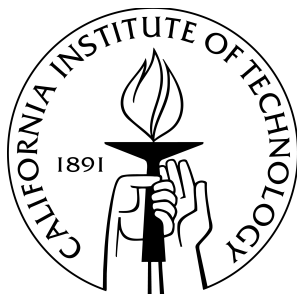
By

Iva Rreza

Submitted to the Department of Chemistry in partial fulfillment of the degree of

BACHELORS IN INORGANIC CHEMISTRY

© 2014 California Institute of Technology. All rights reserved.



CALIFORNIA INSTITUTE OF TECHNOLOGY

Pasadena, California USA 91125

June 2014

Acknowledgements

I would like to express my sincerest gratitude to Professor John Bercaw for his mentorship throughout my project and his inquisitive, encouraging and hands-off teaching style. Professor Doug Rees is also to be thanked for his support and involvement in the senior thesis program. I greatly thank Dr. Aaron Sattler for his co-mentorship in the project, for his very useful suggestions and advice, and for teaching me a great wealth of knowledge in organometallic chemistry. Finally, I would like to extend a big thank you to Professor Harry Gray for including me in the Gray group, for his infectious and encouraging attitude, and for instilling in me an increased interest in inorganic chemistry.

Abstract

The development of catalysts that selectively oligomerize light olefins for uses in polymers and fuels remains of interest to the petrochemical and materials industry. For this purpose, two tantalum compounds, (FI)TaMe₂Cl₂ and (FI)TaMe₄, implementing a previously reported phenoxy-imine (FI) ligand framework, have been synthesized and characterized with NMR spectroscopy and X-ray crystallography. When tested for ethylene oligomerization catalysis, (FI)TaMe₂Cl₂ was found to dimerize ethylene when activated with Et₂Zn or EtMgCl, and (FI)TaMe₄ dimerized ethylene when activated with B(C₆F₅)₃, both at room temperature.

Table of Contents

Title Page	1
Acknowledgements	2
Abstract	3
Table of Contents	4
List of Figures	5
List of Schemes	6

Development of Tantalum Phenoxy-Imine Compounds for Selective Ethylene Oligomerization Compounds

Introduction	7
Synthesis of (FI)H	10
Metalation with Zr	13
Metalation with Ta	15
Synthesis and Characterization of (FI)TaMe ₂ Cl ₂	15
Molecular Structure of (FI)TaMe ₂ Cl ₂	17
Synthesis and Characterization of (FI)TaMe ₄	19
Catalysis with Tantalum Phenoxy-Imine Compounds	23
Conclusions	29
Experimental Methods	30
References	44
Appendix: Supporting Information	37

List of Figures

Figure 1.	Depiction of Cossee Chain Growth trimerization via oligomerization mechanism.	8
Figure 2.	Selective ethylene metallacycle mechanism.	8
Figure 3.	Fujita phenoxy-imine ligand (FI)H.	10
Figure 4.	Structure of the Fujita precatalyst.	10
Figure 5.	Molecular Structure of $Zr(THF)Cl_4$.	14
Figure 6.	X-ray Structure of $(FI)TaMe_2Cl_2$.	17
Figure 7.	Calculated electronic energy of $(FI)TaMe_2Cl_2$ as a function of Me-Ta-Me angle.	18
Figure 8.	Calculated HOMO of $(FI)TaMe_2Cl_2$.	19
Figure 9.	Calculated LUMO of $(FI)TaMe_2Cl_2$.	19
Figure 10.	X-ray structure of $(FI)TaMe_4$.	20
Figure 11.	Manipulated perspective of leftmost structure to depict approximately prismatic geometry at the metal center.	21
Figure 12.	Calculated molecular orbitals of $(FI)TaMe_4$ increasing in energy from left to right: left: MO right below HOMO in energy, middle: HOMO, right: LUMO.	22
Figure 13.	Electronic Spectra of Phenoxy-Imine Compounds.	23
Figure 14.	Proposed conversion of Ta(V) to Ta(III) with one equivalent of $ZnEt_2$ or two equivalents of $EtMgCl$.	24
Figure 15.	Monitoring reaction between $(FI)TaMe_2Cl_2$ and ethylene by 1H NMR spec. Note the olefinic peaks of 1-butene at δ 5.0 and δ 5.8.	26
Figure 16.	1H NMR (600 MHz) spectra of the observed α -olefin along with 1-butene, 1-hexene, and 1-octene.	27
Figure 17.	Reaction of $(FI)TaMe_4$ with $B(C_6F_5)_3$ under the presence of ethylene. Note the very faint olefinic peaks at δ 5.0 and δ 5.8. Note that there is no reaction between $(FI)TaMe_4$ and ethylene alone	28

List of Schemes

Scheme 1.	Synthesis of intermediary compounds in Fujita ligand literature prep. ⁹ a) Synthesis of 2-adamantyl- <i>p</i> -cresol b) Synthesis of 3-adamantyl-2-hydroxy-5-methylbenzaldehyde c) Synthesis of 2-(2'-methoxyphenyl)aniline.	11
Scheme 2.	Synthesis of Fujita Ligand.	12
Scheme 3.	Resulting zwitterionic complex upon reacting $Zr(THF)_2Cl_4$ with (FI)H.	13
Scheme 4.	Proposed reaction of (FI)H and tetrabenzyl zirconium ($ZrBn_4$) to protonate off toluene and generate (FI)ZrBn ₃ .	14
Scheme 5.	Synthesis of TaMe ₃ Cl ₂ .	16
Scheme 6.	Synthesis of (FI)TaMe ₂ Cl ₂ .	16
Scheme 7.	Synthesis of (FI)TaMe ₄ .	20
Scheme 8.	Dimerization of ethylene with (FI)TaMe ₂ Cl ₂ .	25
Scheme 9.	Dimerization of ethylene with (FI)TaMe ₄ .	28

Development of Tantalum Phenoxy-Imine Compounds for Selective Ethylene Oligomerization

Introduction

Prevalent as intermediates in today's synthesis of detergents, lubricants, packaging materials and other such common synthetic products, linear α -olefins (LAOs) are a ubiquitous industrial source.¹ Annually, energy companies such as Ineos, Shell, and Chevron collectively manufacture millions of tons of LAOs. A significant portion of the light fraction LAOs (C₄-C₈) today undergoes copolymerization with ethylene to produce linear low-density polyethylene (LLDPE).¹ In this context, 1-butene, 1-hexene, and 1-octene are used to control the density and to impart desirable properties such as good tear resistance to the polymer.² The increasing demand of LLDPE products stipulates the ability to generate light α -olefins as selectively and efficiently as possible. For this purpose, academic and industrial efforts in the development of selective oligomerization systems are ongoing.¹ In addition to imparting selectivity, it is important also that these systems must not isomerize the final α -olefin to the more stable internal olefins; internal olefins are less reactive than their terminal olefin counterparts and build up in polymerization reactions.

Synthesis of LAOs from ethylene (C₂H₄) by metal-catalyzed olefin oligomerization methods is the current state of the art, but problems like poor selectivity for the α -olefin of choice remain. Consequently, this challenge has sparked significant research efforts toward the search for improved ethylene oligomerization routes. As of now, there are only several commercialized selective oligomerization processes for ethylene dimerization (Alphabutol), trimerization (Chevron Phillips, IFP), and tetramerization (Sasol).¹ Given the industrial value of selective oligomerization methods, it is of importance to understand the mechanistic basis for selectivity.

A test distinguishing between a Cossee and metallacycle mechanism was developed initially in studying the mechanism of 1-butene formation for a $\text{Ti}(\text{OC}_4\text{H}_9)_4\text{-AlR}_3$ system.⁴ In this study, a codimerization of protio and deuterio ethylene with the catalyst was performed to reveal: 1) the rate-limiting step in 1-butene formation is β -H elimination and 2) the mechanism of formation resembled a Cossee-like mechanism. Essentially, the isotopologue distribution resulting from a 1:1 mixture of ethylene and d_4 -ethylene indicates one mechanism over the other on the basis of H/D scrambling. The Cossee mechanism yields a distribution of isotopologues with odd numbers of hydrogen and deuterium atoms while the metallacycle mechanism does not lead to scrambling. In other words, the system should have yielded C_4H_8 , $\text{C}_4\text{H}_4\text{D}_4$, and C_4D_8 if a metallacycle mechanism was responsible, but instead yielded a distribution of 1-butene molecules with molecular masses ranging from 56 to 64.⁴ In 2004, Bercaw and co-workers utilized this test to distinguish between the Cossee and metallacycle mechanism in their investigation of a chromium ethylene trimerization system.⁵ They concluded that a selective trimerization system undergoes a metallacycle mechanism.

Whereas the metallacycle mechanism is strictly invoked in selective trimerization and tetramerization routes, mechanistic studies for selective dimerization, interestingly, provide evidence for multiple routes (i.e. Cossee and metallacycle). The mechanistic test described above has been done for other titanium alkoxide catalysts, similar to the one used in the Alphabutol process. For these catalysts, a distribution of H/D scrambled isotopomers has been observed, implying a Cossee type mechanism.¹

The most widely studied metal for trimerization catalysis is Cr, but Ti, V, and Ta have also been reported as viable catalysts. Recently, a new titanium catalyst reported by Fujita and coworkers (Figure 4) has garnered interest for its incredible activity and selectivity towards trimerizing ethylene to produce 1-hexene.⁶ Like several chromium catalysts,² the Fujita catalyst is believed to proceed through a metallacycle mechanism, having activities of 6000 kg of 1-hexene per gram of catalyst per hour with 99% yield.⁶ The selectivity varies

with conversion; at high conversion, co-trimerization of 2 ethylenes with 1-hexene occurs to give a C₁₀ product.

One of the defining features of the structure of the Fujita catalyst is the large, organic ligand, part of a class of ligands known as phenoxy-imine (FI) ligands (Figure 3). In the 1990s, it was discovered that certain phenoxy-imine ligands serve very well for olefin insertion/polymerization catalysts with early and late transition metals.⁷ Extensive research and ligand optimization has extended the functionality of FI compounds with late transition metals like Ni to ethylene oligomerization,⁸ and such as in the case of the Fujita system, with an early transition metal like Ti as well.

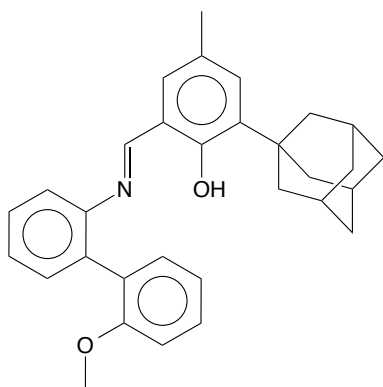


Figure 3. Fujita phenoxy imine ligand (FI)H.

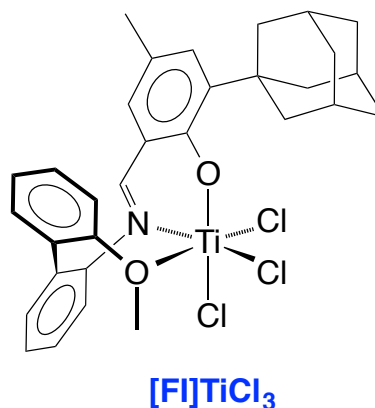


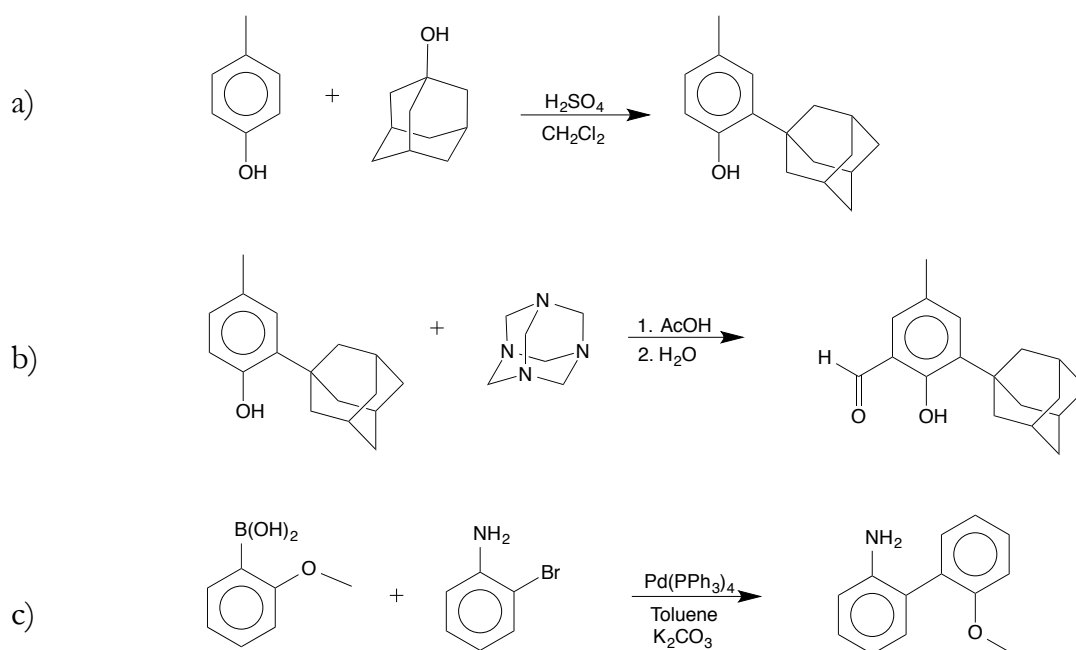
Figure 4. Structure of the Fujita precatalyst.

Employing the same phenoxy-imine ligand framework present in the Fujita system, this study presents two new tantalum phenoxy-imine compounds that dimerize ethylene.

Synthesis of the Fujita Ligand: (FI)H

Previous members of the Bercaw group have modified the original literature synthesis of the Fujita ligand (FI)H for more optimized yields. For the purposes of this study, the synthesis of the FI ligand was scaled up from the most recent literature synthesis and

modified to obtain 10 g of pure FI ligand (Yield: 57%).⁹ Considering the demand for the ligand during this study, improving yields of intermediary steps and scaling up ligand synthesis was deemed necessary. Under these modifications, yields of several intermediary compounds were improved. The FI ligand is synthesized in four steps to make 1) 2-adamantyl-*p*-cresol 2) 3-adamantyl-2-hydroxy-5-methylbenzaldehyde 3) 2-(2-methoxyphenyl)aniline and finally the ligand, (FI)H (see Experimental Methods). Beginning with *p*-cresol, 2-adamantyl-*p*-cresol is formed by means of an aromatic substitution reaction with adamantanol, to obtain an adamantyl group in the ortho position (Scheme 1a). This is further treated with hexamethylenetetraamine (HMTA) to undergo formylation. (Scheme 1b)

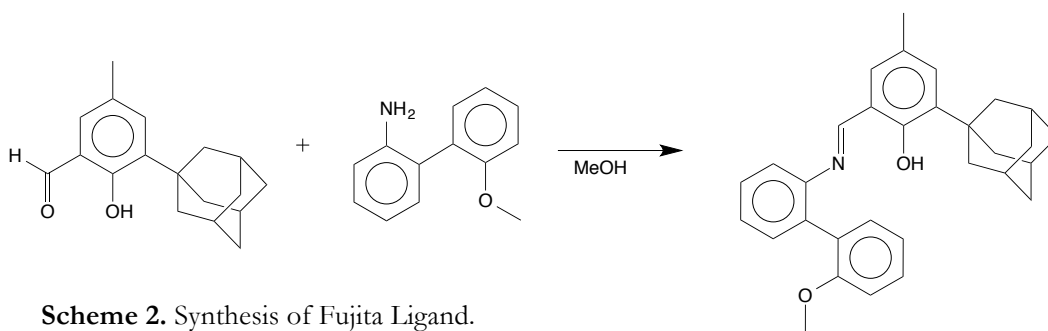


Scheme 1. Synthesis of intermediary compounds in Fujita ligand literature prep.⁹ a) Synthesis of 2-adamantyl-*p*-cresol b) Synthesis of 3-adamantyl-2-hydroxy-5-methylbenzaldehyde c) Synthesis of 2-(2-methoxyphenyl)aniline.

One synthetic focus in the scale-up was this particular formylation reaction (Duff reaction) to make the benzaldehyde, as previous attempts have proved difficult in isolating

the precipitated product. It was observed that immediate addition of water to the orange solution in acetic acid to precipitate the desired product results in the formation of a very compact orange solid that gathers at the bottom of the flask and is insoluble in organic solvents. This may be a result of a polymerization type reaction with unreacted HMTA and high concentrations of water. The use of an addition funnel to transfer water also results in the formation of this orange, insoluble solid. We found instead that if 0.25 equivalents of water are added and the solution stirred overnight, the orange solid does not form. This method allows the procedure to be scaled up from 5 grams to 10 grams (previous attempts at 10 gram reactions resulted in low yields (< 10 %) and difficulties with isolation) to obtain a fine off-white solid precipitate. Our yield was 5.6 grams, yield: 63%, which is an improvement from the literature yield of 52%.

The literature synthesis of the aniline, consisting of a Suzuki coupling of 2-methoxyphenylboronic acid and 2-bromoaniline (Scheme 1c), was also modified. It was observed on previous attempts that the reaction was incomplete after heating for 18 hours, and further heating did not result in increased yields. A 15% addition of the coupling catalyst, Pd(PPh₃)₄, however, resulted in an improved yield of 65%, compared with the previous report of 40%.⁹



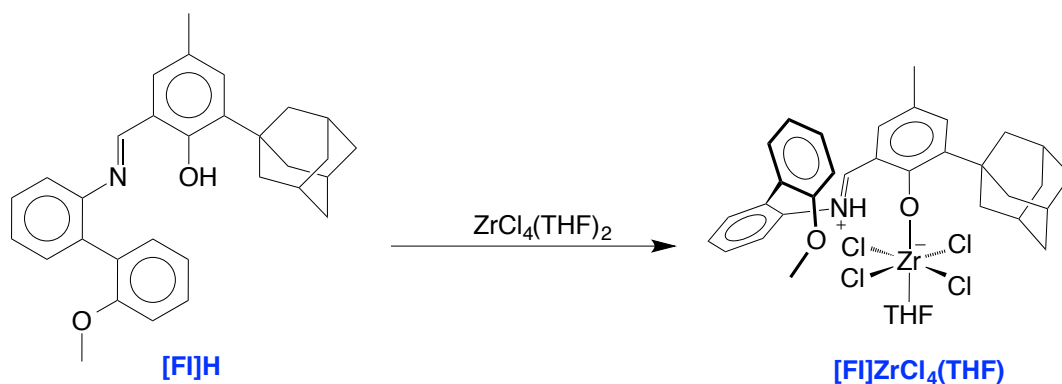
Scheme 2. Synthesis of Fujita Ligand.

Combining the aniline product with 3-adamantyl-2-hydroxy-5-methylbenzaldehyde (Scheme 2) yielded close to 10 g of pure (FI)H ligand in the largest scale synthesis attempt. The ¹H NMR of the ligand in CDCl₃ denotes the main structural moieties: the Ar-OH peak

(δ 13.5), the imine peak (N=CH, δ 8.5), and the aryl methoxy peak (OMe, δ 3.75) (see Appendix Figure A11).

Metalation with Zirconium

Zirconium was the initial metal of choice for metalation of the (FI)H ligand. Although there are no reported oligomerization systems with zirconium, systems with titanium, zirconium's lighter congener, have been previously reported as selective trimerization precatalysts.^{6,10} In addition, theoretical studies performed on $[(\eta^5\text{-C}_5\text{H}_4\text{-(CMe}_2\text{-bridge)-C}_6\text{H}_5)\text{M}^{\text{IV}}(\text{CH}_3)_2]^+$ suggest faster metallacycle growth for Zr than Ti,¹¹ indicating a higher potential activity for Zr. For this reason, we aimed to synthesize (FI)ZrCl₃, the Zr equivalent of the Fujita catalyst, hoping to discover a new catalyst system. In an effort to synthesize (FI)ZrCl₃, (FI)H was reacted with the *bis*-THF zirconium tetrachloride, Zr(THF)₂Cl₄, precursor. Unfortunately, this afforded an interesting but undesired zwitterionic compound, namely [(FI)H']ZrCl₄(THF) (H' denotes that the H is coordinated to the imine nitrogen) (Scheme 3), which was structurally characterized by X-ray crystallography (Figure 5). We postulated that the reaction should eliminate HCl to produce the desired phenoxy-imine Zr complex, (FI)ZrCl₃, but HCl evolution was not observed.



Scheme 3. Resulting zwitterionic complex upon reacting Zr(THF)₂Cl₄ with (FI)H.

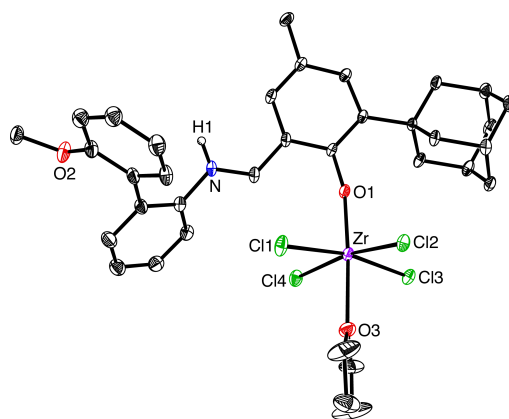
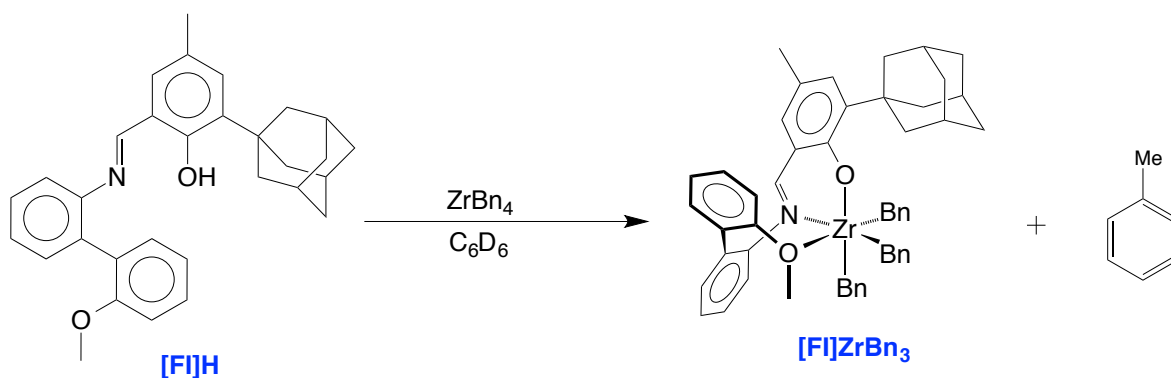


Figure 5. Molecular Structure of (FI)Zr(THF)Cl₄.

Metalation was then attempted with the deprotonated ligand, like many literature syntheses report. Deprotonation and hence synthesizing the corresponding phenoxide was performed n-butyl lithium (BuⁿLi) and potassium hydride (KH). However, this method yielded mixtures of complexes. The precursor was varied also to a tetrabenzyl zirconium (ZrBn₄) compound which when reacted with (FI)H should eliminate toluene to yield (FI)ZrBn₃. (Scheme 4) However, this resulted in a complex mixture of unreacted and reacted product as well as potential bis-ligand compounds, which were identified by ¹H NMR spectroscopy. (see Appendix Figure A12)



Scheme 4. Proposed reaction of (FI)H and tetrabenzyl zirconium (ZrBn₄) to protonate off toluene and generate (FI)ZrBn₃.

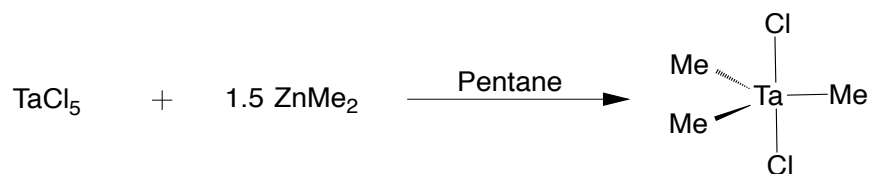
Metalation with Tantalum

While there are no reported ethylene oligomerizing systems with zirconium, there are several tantalum systems known to selectively oligomerize ethylene.^{12, 13, 14} Various tantalacyclopentane catalytic systems reported by Schrock¹² selectively dimerize ethylene (and α -olefins). Interestingly, ethylene binds to these compounds to form more stable metallacycles than higher α -olefins. As a result, the rate of dimerization of ethylene is considerably slower than that of α -olefins for these systems. Schrock's study proposes a mechanism of dimerization whereby the metalocyclopentane ring contracts to a metalocyclobutane ring that then eliminates to form 1-butene.¹² Tantalum systems that have been reported to trimerize ethylene with high specificity are thought to proceed through a Ta(III) catalytic intermediate. For example, in the case of the Sen and coworkers¹³ study, pentachlorotantalum(V) (TaCl_5) was treated with various alkylating agents (MeLi , Et_2Zn , etc.) to produce a putative trichlorotantalum(III) (TaCl_3) that then trimerizes ethylene, with greater than 98% selectivity. They believe this occurs through a metallacycle mechanism. Mashima and coworkers,¹⁴ also report a highly selective tantalum trimerization system that activates TaCl_5 with 3,6-*bis*(trimethylsilyl)-1,4-cyclohexadiene (BTCDD) instead to achieve ligandless Ta(III). Although highly selective, these catalysts are relatively short lived and inefficient, with turnover numbers of 500 (Sen and coworkers) and 1000 (Mashima and coworkers) mol ethylene per mol of Ta per hour.

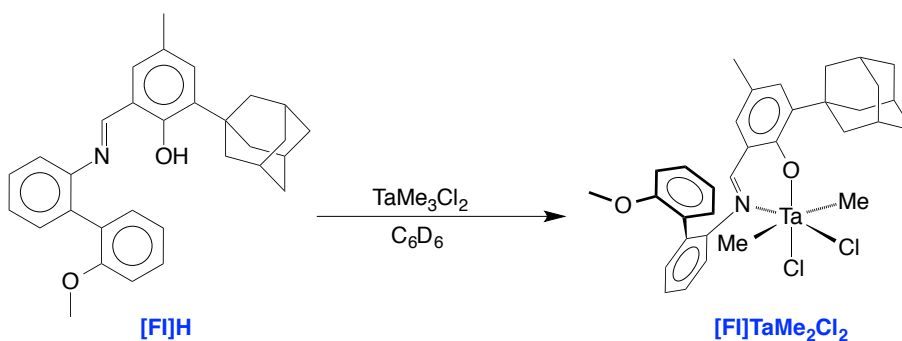
Synthesis and Characterization of (FI)TaMe₂Cl₂

Once Zr proved futile, metalation efforts shifted towards tantalum. Tantalum trimethyl dichloride (TaMe_3Cl_2), similar to the precatalyst in the Sen Study (TaMe_2Cl_3), was synthesized as a metal precursor from literature synthesis¹⁵ (Scheme 5) with the hopes of

protonating off methane when treated with (FI)H. This would free up coordination sites at the metal center and encourage proper FI binding to the metal center. Indeed, upon reacting (TaMe₃Cl₂) with (FI)H in deuterobenzene (C₆D₆), (FI)TaMe₂Cl₂ (and methane) forms, as observed by ¹H NMR spectroscopy (see Appendix). (FI)TaMe₂Cl₂ has been characterized by ¹H NMR, ¹³C NMR, X-ray crystallography and elemental analysis. By ¹H NMR, characteristic functional groups are located at δ1.58 (TaMe₂), δ3.10 (OMe), and δ8.33 (C=NH). Respective to their chemical shifts on the pure ligand (δ3.75 and δ8.5), the methoxy and imine peaks have clearly shifted, indicating metalation. In addition, a single ¹H NMR peak indicates chemically equivalent methyl groups on the molecule on NMR timescale.



Scheme 5. Synthesis of TaMe₃Cl₂.



Scheme 6. Synthesis of (FI)TaMe₂Cl₂.

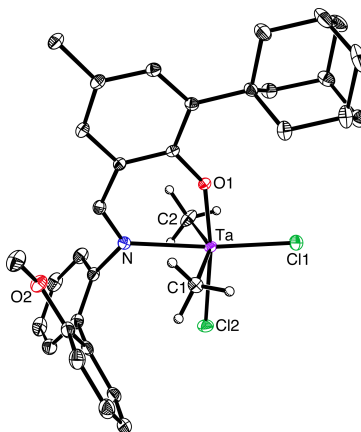


Figure 6. X-ray Structure of (FI)TaMe₂Cl₂.

Molecular Structure of (FI)TaMe₂Cl₂

As demonstrated by the crystal structure of (FI)TaMe₂Cl₂ (Figure 6), the compound is subtly and interestingly non-octahedral and 6-coordinate. The defining feature of this geometry can be seen in the Me₁-Ta-Me₂ angle, which is not 180°, but in fact 153.9°. The methyl groups are seemingly pointing towards some of the steric bulk of ligand. If not for the discrepancy in bond angle to around 170° in another crystal derived from C₆D₆, this peculiarity suggests the possibility of stabilizing agostic interactions. Taking into account the discrepant angle, however, it seems more likely that the underlying cause is a more common crystal packing effect. To investigate the distortion of the Me-Ta-Me angle in (FI)TaMe₂Cl₂ away from 180° (ideal angle for octahedral), DFT calculations (Jaguar, Schrodinger LLC) were conducted. Geometry optimization calculations of (FI)TaMe₂Cl₂, in addition to relaxed optimizations with fixed Me-Ta-Me angles, gave indication that the distortion observed in the X-ray crystal structure was not a solid-state or crystal packing effect. In fact, the optimized angle is 147.8°. Figure 7 shows the normalized energy with respect to an incremental angle (increments of 5) energy analysis (kcal/mol). Computationally, the molecule prefers a Me₁-Ta-Me₂ angle of 147.8°. The reason for this distortion is not fully understood yet, but could still perhaps indicate the presence of a stabilizing agostic interaction between the hydrogen atoms on the methyl groups and the metal center.

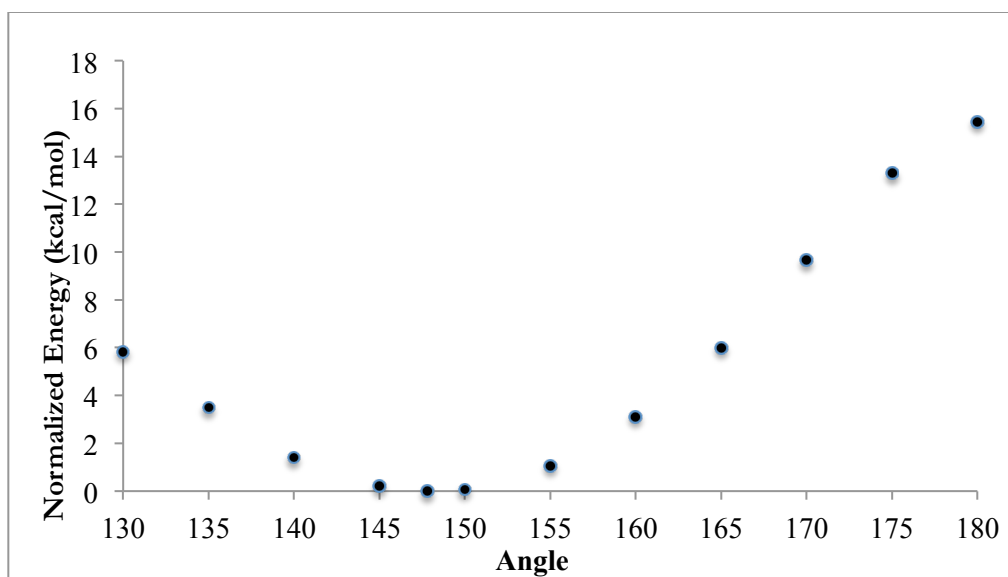


Figure 7. Calculated electronic energy of (FI)TaMe₂Cl₂ as a function of Me-Ta-Me angle.

The electronic spectrum of (FI)TaMe₂Cl₂ was obtained using UV-Vis spectroscopy in C₆D₆ to reveal a faint, broad band at around 360 nm. Since the tantalum metal center has an oxidation number of five and hence no d electrons, d-d transitions can immediately be ruled out as the cause of any observed bands. Instead, the bands must originate from a charge transfer band. As such, the band may either represent a ligand-to-metal charge transfer (LMCT) or a ligand-to-ligand charge transfer. Intense ligand to metal charge transfer occur when there is a high probability of electronic transition from a σ or π ligand orbital or an orbital of ligand character to (in this case) an empty metal orbital. The charge transfer transition is responsible for the orange color of (FI)TaMe₂Cl₂. Molecular orbital analyses were performed with the aid of Jimp2,¹⁶ which employs Fenske-Hall calculations and visualization using MOPLLOT.¹⁷ Analyses revealed that the highest occupied molecular orbital (HOMO) of the molecule is localized predominantly around the FI ligand and resembles ligand π orbitals. (Figure 8) The lowest unoccupied molecular orbital (LUMO) on the other hand is localized on the metal center and resembles a d_{yz} orbital (Figure 9). This

may indicate to some extent that the charge transfer resembles a ligand-to-metal one but as the geometry of the molecule is non-ideal, it is unclear.

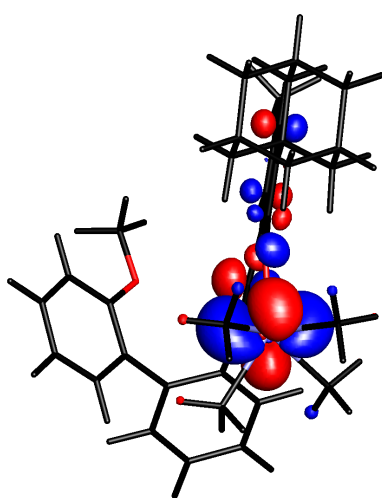


Figure 8. Calculated HOMO of (FI)TaMe₂Cl₂.

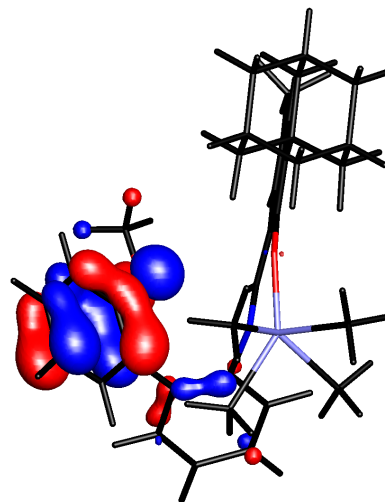


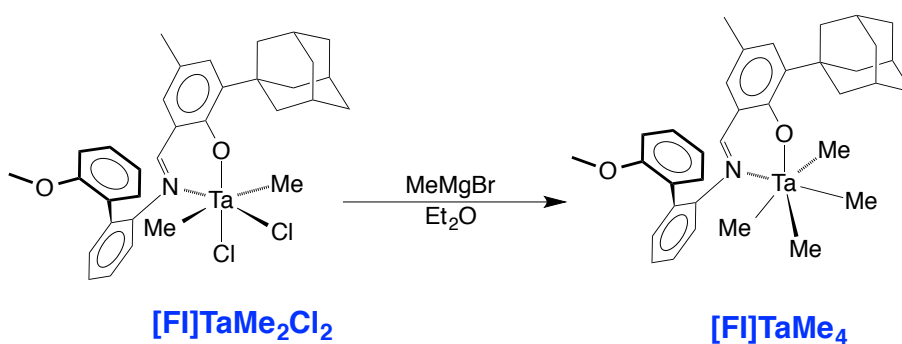
Figure 9. Calculated LUMO of (FI)TaMe₂Cl₂.

Synthesis and Characterization of (FI)TaMe₄

After synthesizing (FI)TaMe₂Cl₂, it was of interest to attempt to synthesize its tetramethyl analogue (FI)TaMe₄. To date, there are only a handful of reported tantalum tetramethyl compounds as well as pentamethyl and hexamethyl.^{18,19,20,21} This includes Cp*Ta(CH₃)₄¹⁹, a tantalum-borollide alkyl complex ([η^5 - C₄H₄BN(CNMe₂)₂]Me₂Ta-[μ -n⁵-C₄H₄BN(CHMe₂)₂]TaMe₄)¹⁸, Ta(CH₃)₅²¹, and Ta(CH₃)₆²⁰. Tantalum tetramethyl and pentamethyl compounds tend to exhibit limited thermal stability^{18,19,21} and are often handled at low temperatures (i. e. below -30°C).

(FI)TaMe₄ was made by treating (FI)TaMe₂Cl₂ with 2 equivalents of MeMgBr in Et₂O, affording a yellow compound. (Scheme 7) With ZnMe₂, a milder methylating agent,

(FI)TaMe₂Cl₂ fails to form (FI)TaMe₄. X-ray worthy crystals were obtained by crystallizing a solution of the compound in Et₂O at -35°C. (Figure 10) Taking ¹H NMR spectra of the resulting crystals reveals the characteristic functional groups of the ligand (δ 2.80 OMe, δ 8.43 C=NH) that have shifted from their original location, again indicating metalation. In addition, the methyl groups of the compound are observed as a singlet (δ 1.23), indicating chemical equivalence. Like its parent compound, (FI)TaMe₄ is non-octahedral but resembles a pseudo trigonal prismatic geometry. (Figure 11)



Scheme 7. Synthesis of (FI)TaMe₄.

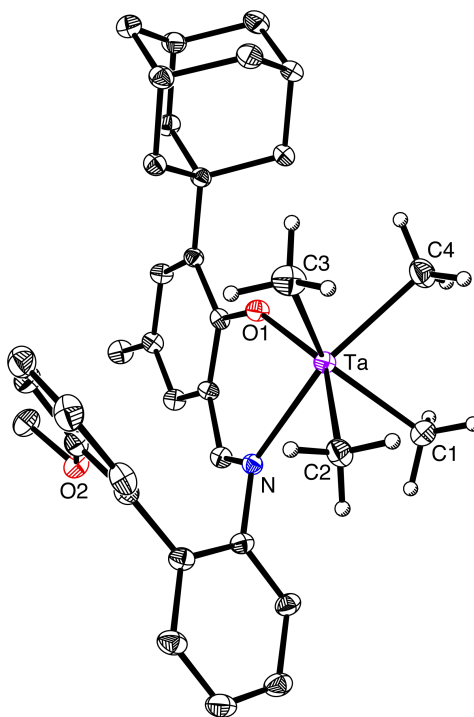


Figure 10. X-ray structure of (FI)TaMe₄.

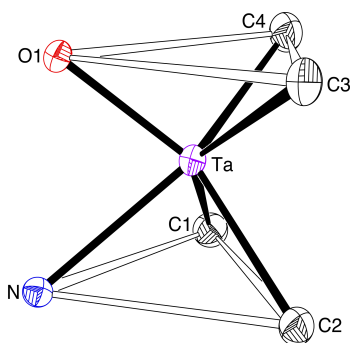


Figure 11. Manipulated perspective of leftmost structure to depict approximately prismatic geometry at the metal center.

Initially, the consistent isolation of the compound as well as a scaled up synthesis proved difficult. Addition of excess MeMgBr to (FI)TaMe₂Cl₂ results in the formation of dark green crystalline material, which is highly sensitive to moisture and oxygen. Several attempts have been made to obtain the molecular structure of this product, but all have been unsuccessful as exposure to air causes the crystals to smoke immediately and sometimes ignite. It is postulated that an “ate” complex is forming in this case, in which the excess MeMgBr overalkylates, forming a compound such as (FI)TaMe₅⁻. Anionic “ate” complexes of tantalum have been previously reported.²⁰ Fortunately, the addition of dioxane after MeMgBr during synthesis has allowed for the isolation of pure (FI)TaMe₄ (Yield: 42%). Dioxane (C₂H₄O)₂ reacts with Grignard reagents to precipitate the resulting magnesium salts out of solution by forming a complex: MgX₂(C₂H₄O)₂ (X = Cl, Br).

The electronic spectrum of (FI)TaMe₄ was obtained using UV-Vis spectroscopy in C₆D₆ to reveal a broad and intense band at around 375 nm. Molecular orbital analyses were performed as well with the aid of Jimp2,¹⁶ which employs Fenske-Hall calculations and visualization using MOPLLOT.¹⁷ Interestingly, as with (FI)TaMe₂Cl₂, the calculated HOMO of (FI)TaMe₄ is very heavily ligand-based and localized on the ligand, while the LUMO is predominantly metal-based. (Figure 12) In addition, the HOMO-LUMO energy gap for (FI)TaMe₂Cl₂ is greater than that of (FI)TaMe₄ by less than 1eV. While we cannot directly

attribute the color of the complexes to any particular charge transfer band (LMCT or LLCT), there is a correlation between the shade of color of the complex and varying amounts of chloride ligands. For example, (FI)TiCl₃ is red in color while (FI)TaMe₂Cl₂ is orange and (FI)TaMe₄ yellow. Perhaps chloride contribution to the metal center biases the complex towards the more reddish hues. In addition, the molecular orbital closest in energy to the HOMO has considerable character on one of the chloride ligands. (Figure 12). Finally, the electronic spectrum of the Fujita ligand ((FI)H) was obtained in C₆D₆ to reveal a broad and intense peak at 360 nm, similar in location to that of (FI)TaMe₄ and (FI)TaMe₂Cl₂ (Figure 13). This final evidence rules in favor of ligand to ligand charge transfer character for the respective bands of each complex, but may not explain the varying colors of the complexes as they all possess the same FI ligand.

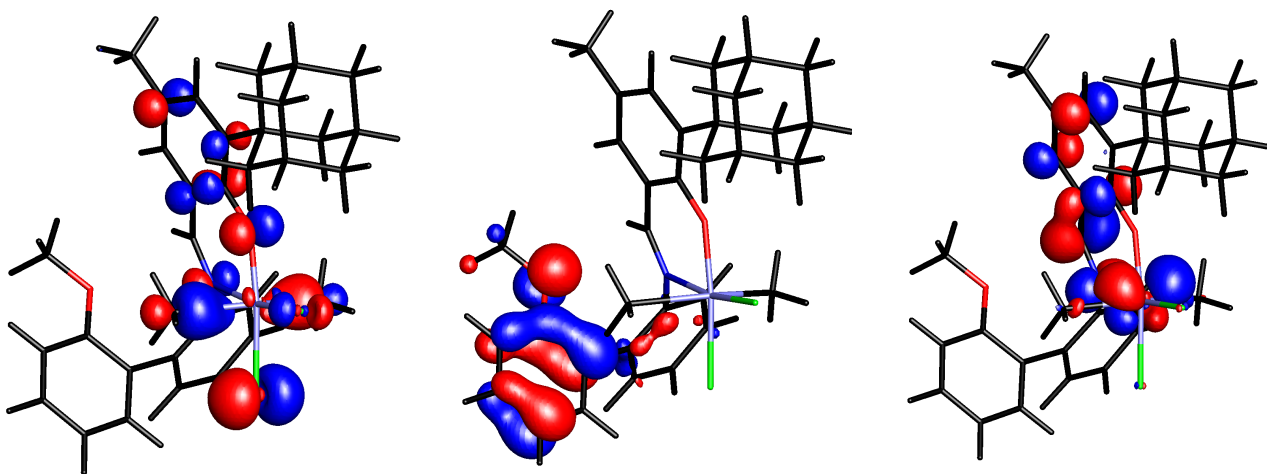


Figure 12. Calculated molecular orbitals of (FI)TaMe₄ increasing in energy from left to right: left: MO right below HOMO in energy, middle: HOMO, right: LUMO.

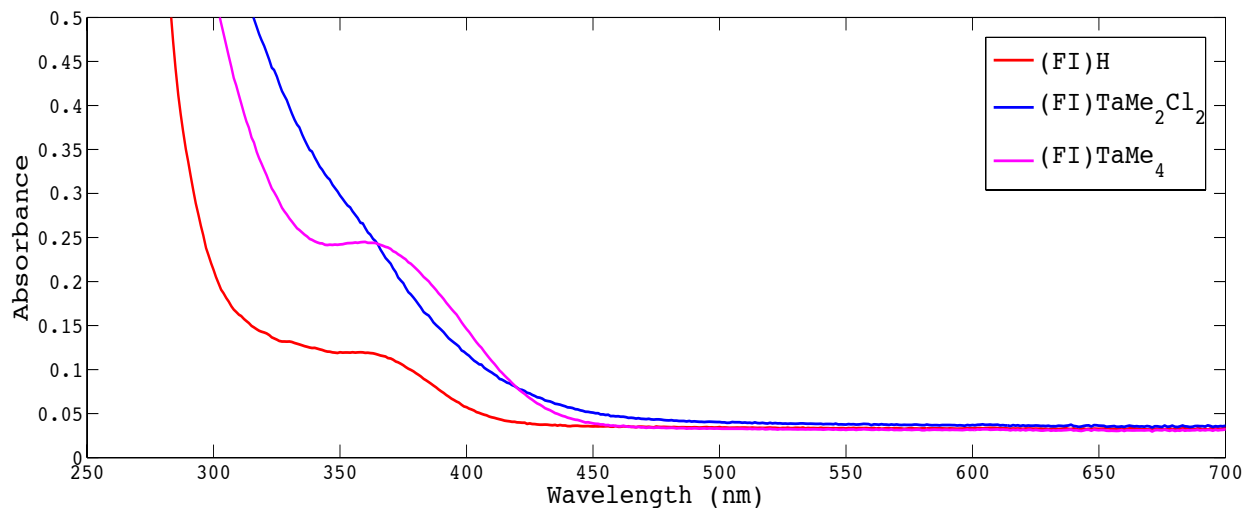


Figure 13. Electronic Spectra of Phenoxy-Imine Compounds.

Catalysis with Tantalum Phenoxy-Imine Compounds

While (FI)TiCl₃ is sometimes denoted as the Fujita “catalyst”, in reality this compound is a precatalyst. The Fujita system employs methylaluminumoxane (MAO), an ill-defined molecule, at ratios of 1:10,000 (catalyst:MAO). Essentially, MAO abstracts chloride ligands from (FI)TiCl₃ to generate a Ti(II) catalytic species that inserts ethylene and undergoes the metallacycle mechanism to generate 1-hexene.⁶ In many cases, what is often denoted as a “catalyst” is really a precatalyst, and thus it is necessary to consider the nature of the active catalytic species and ways in which the precatalyst may be activated. Considering the Mashima¹⁴ and Sen¹³ studies (see Metalation with Tantalum section), we presumed that our system must attain a Ta(III) species before it performs catalysis. To encourage this conversion, various alkylating agents, like in the Sen study, and other activating agents were used to activate the compound. Each activating agent would propose differing routes of activation. Ethyl magnesium chloride (EtMgCl) as well as diethyl zinc (ZnEt₂), for example, could substitute the chloride ligands with ethyl groups on (FI)TaMe₂Cl₂ to form (FI)Ta^VMe₂Et₂ which could undergo β-hydrogen elimination to create

(FI)Ta^VMe₂(C₂H₄)(H)Et. Poised for reductive elimination, this complex could then rapidly reductively eliminate methane to generate (FI)Ta^{III}Me(Et)(C₂H₄), the desired Ta(III) species for trimerization (Figure 14).

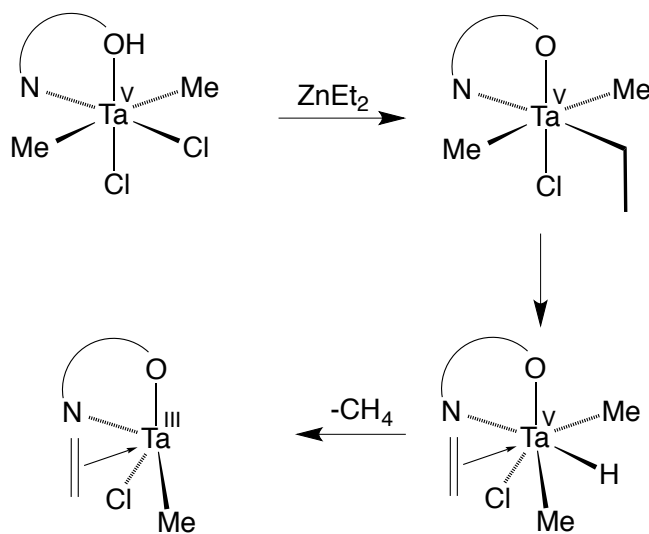
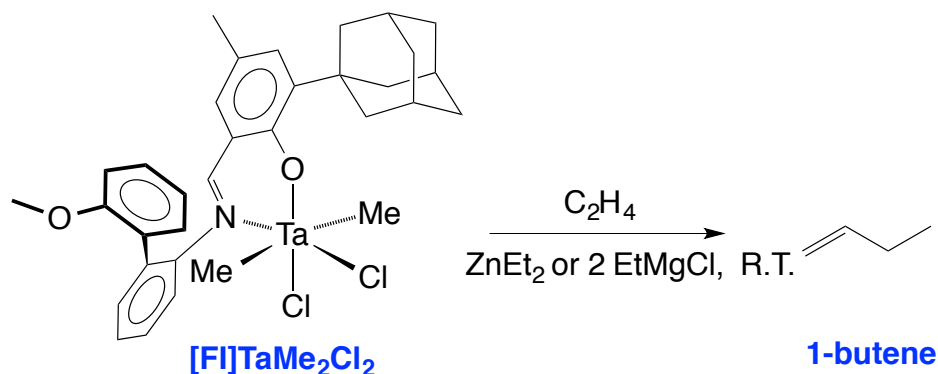


Figure 14. Proposed conversion of Ta(V) to Ta(III) with one equivalent of ZnEt₂ or two equivalents of EtMgCl.

Through a substantially different mechanism, one equivalent of tris(pentafluorophenyl) borane (B(C₆F₅)₃) could abstract a methyl group from (FI)TaMe₂Cl₂ and generate the species [(FI)TaMeCl₂][(H₃C)B(C₆F₅)₃] which although not Ta(III) could facilitate ethylene coordination to the metal center and promote oligomerization. Trityl tetrakis(pentafluorophenyl)borate ([Ph₃C]⁺[B(C₆F₅)₄]⁻, trityl borate), another strong Lewis acid, should have a similar effect to B(C₆F₅)₃ to generate [(FI)TaMeCl₂]⁺ [B(C₆F₅)₄]⁻ + Ph₃C(CH₃). PROTON sources like dimethylanilinium tetrakis(pentafluorophenyl) borate should protonate off methane and generate the same species as that of trityl borate and B(C₆F₅)₃ along with dimethyl aniline. Finally, the methyl derivative of the silane used in the Mashima study (MBTCD) was also proposed as an activating agent to determine if a similar effect to TaCl₅ would be observed (i. e. reduce the metal center by abstracting chloride ligands to generate Ta(III) and observe oligomerization).

When (FI)TaMe₂Cl₂ was activated separately with B(C₆F₅)₃, trityl borate and anilinium borate in the presence of ethylene, no oligomers were observed by ¹H NMR spectroscopy. Activating with anilinium borate in the presence of ethylene surprisingly exhibited almost no change to a new compound. Activating with trityl borate also under the presence of ethylene showed little change, namely slight shifts in the imine proton (δ 8.33 to δ 8.26) and methoxy group (δ 3.10 to δ 3.05) and some obscuration of other ligand peaks. The addition of MBTCD to (FI)TaMe₂Cl₂ unfortunately had no effect on the complex by ¹H NMR spectroscopy.

Fortunately, 1-butene forms in solution upon activating (FI)TaMe₂Cl₂ under ethylene (1 atm) with an excess (or 1 equivalent) of ZnEt₂ as well as separately with 2 equivalents of EtMgCl. This is significant as the reactions occur at room temperature, while most other catalysts require elevated temperatures. Further characterization is needed to determine exactly how catalysis occurs.



Scheme 8. Dimerization of ethylene with (FI)TaMe₂Cl₂.

As discussed above, we believed initially that addition of Et₂Zn, or 2 equivalents of EtMgCl, would replace the chlorines with ethyl groups, which can then β-hydride eliminate to make an ethylene hydride complex, and further reductively eliminate methane and produce the Ta(III) complex. However, ¹H NMR spectroscopic studies indicated that an

exchange reaction between the ethyl and methyl groups occurred, rather than the chlorides, as evidenced by formation of ZnMe_2 (broad peak at $\delta -0.67$). Monitoring the reaction by ^1H NMR spectroscopy (Figure 15) elucidates a few noteworthy observations: the olefinic peaks of 1-butene, the broad and shifting peak below zero intimating fast alkyl exchange to form some type of zinc methyl compound, the formation of ethane ($\delta = 0.80$), and the disappearance of $(\text{FI})\text{TaMe}_2\text{Cl}_2$ peaks upon activation. It should be noted that the olefinic peaks of 1-butene, 1-hexene, and 1-octene lie in close proximity in ^1H NMR spectra. Spectra of these α -olefins were closely compared at the same field frequency to reveal an almost perfect match of the experimentally observed α -olefin and 1-butene.

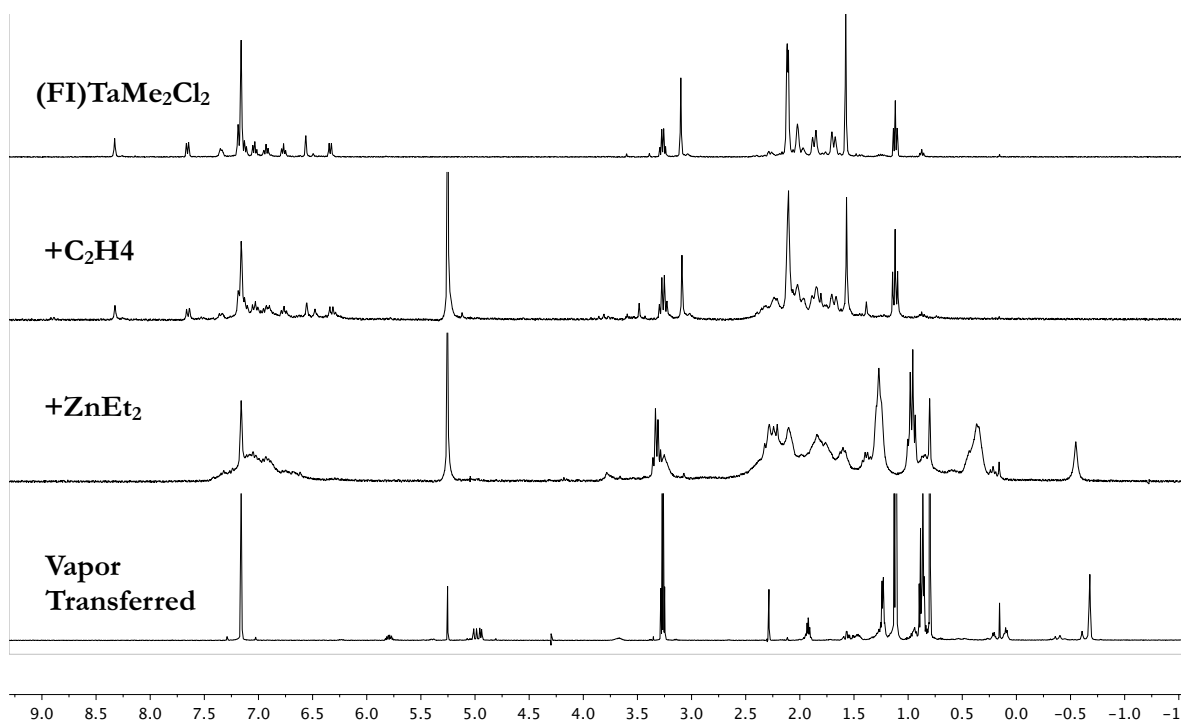


Figure 15. Monitoring reaction between $(\text{FI})\text{TaMe}_2\text{Cl}_2$ and ethylene by ^1H NMR spec. Note the olefinic peaks of 1-butene at δ 5.0 and δ 5.8.

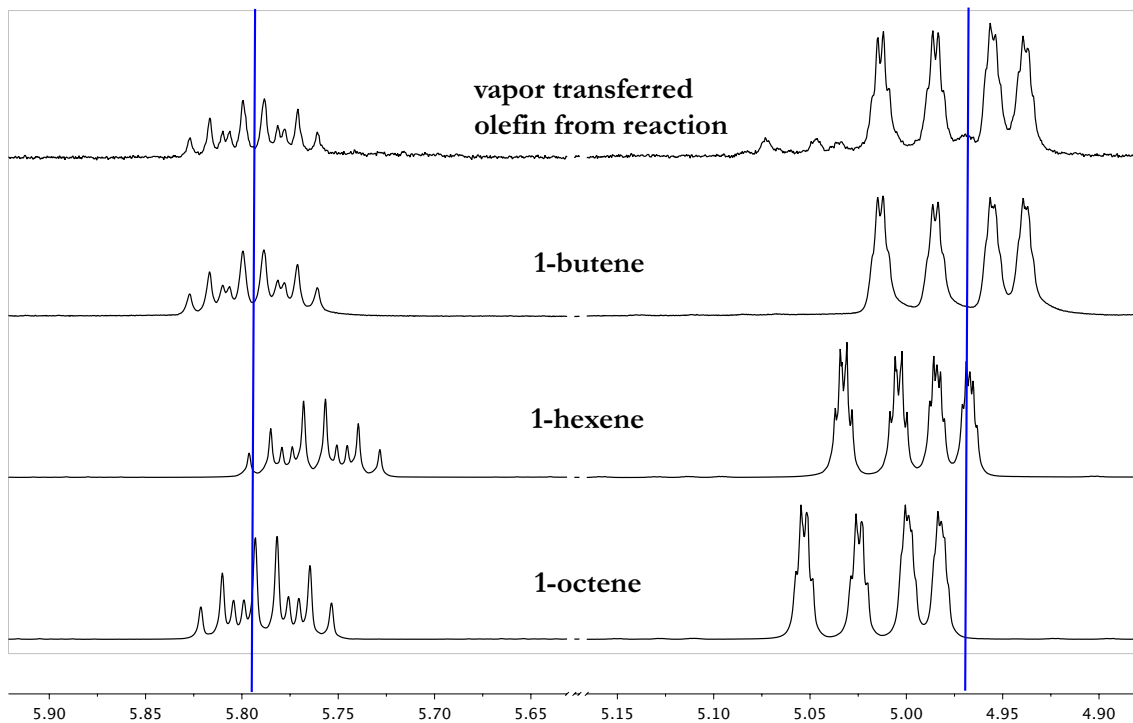
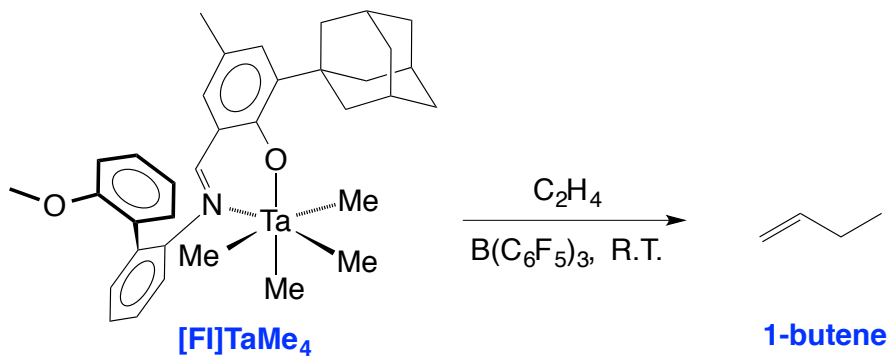


Figure 16. ^1H NMR (600 MHz) spectra of the observed α -olefin along with 1-butene, 1-hexene, and 1-octene.

As with $(\text{FI})\text{TaMe}_2\text{Cl}_2$, the ethylene oligomerization capabilities of $(\text{FI})\text{TaMe}_4$ have been explored with various activating agents. When treated with one equivalent of $\text{B}(\text{C}_6\text{F}_5)_3$ under the presence of ethylene at room temperature, (presumably to yield $[(\text{FI})\text{TaMe}_3][\text{MeB}(\text{C}_6\text{F}_5)_3]$) $(\text{FI})\text{TaMe}_4$ is observed to also dimerize ethylene. (Scheme 9) By ^1H NMR, $(\text{FI})\text{TaMe}_4$ shows full conversion to a new compound with one eq. of $\text{B}(\text{C}_6\text{F}_5)_3$. This is seen most clearly with new peaks at δ 7.95 (imine proton of the FI ligand), δ 3.17 (a shifting methoxy peak from δ 2.80 that could indicate coordination to the metal center) (Figure 17). It is unclear what the activated species is that is involved in oligomerization. Crystallizing the compound formed from treating $(\text{FI})\text{TaMe}_4$ with one equivalent of $\text{B}(\text{C}_6\text{F}_5)_3$ has also proved unsuccessful. In addition, dimerizing ethylene with $(\text{FI})\text{TaMe}_4$ and $\text{B}(\text{C}_6\text{F}_5)_3$ has exhibited some difficulty in reproducibility. Similar to $\text{B}(\text{C}_6\text{F}_5)_3$, trityl tetrakis(pentafluorophenyl) borate may also prove a worthy methyl abstracting agent and activator. Dimethylanilinium tetrakis(pentafluorophenyl) borate was tested for its ability to

activate (FI)TaMe₄. Unfortunately, no olefins were detected, but a new compound was observed by ¹H NMR spectroscopy, somewhat similar to that achieved with one equivalent of B(C₆F₅)₃.



Scheme 9. Dimerization of ethylene with (FI)TaMe₄.

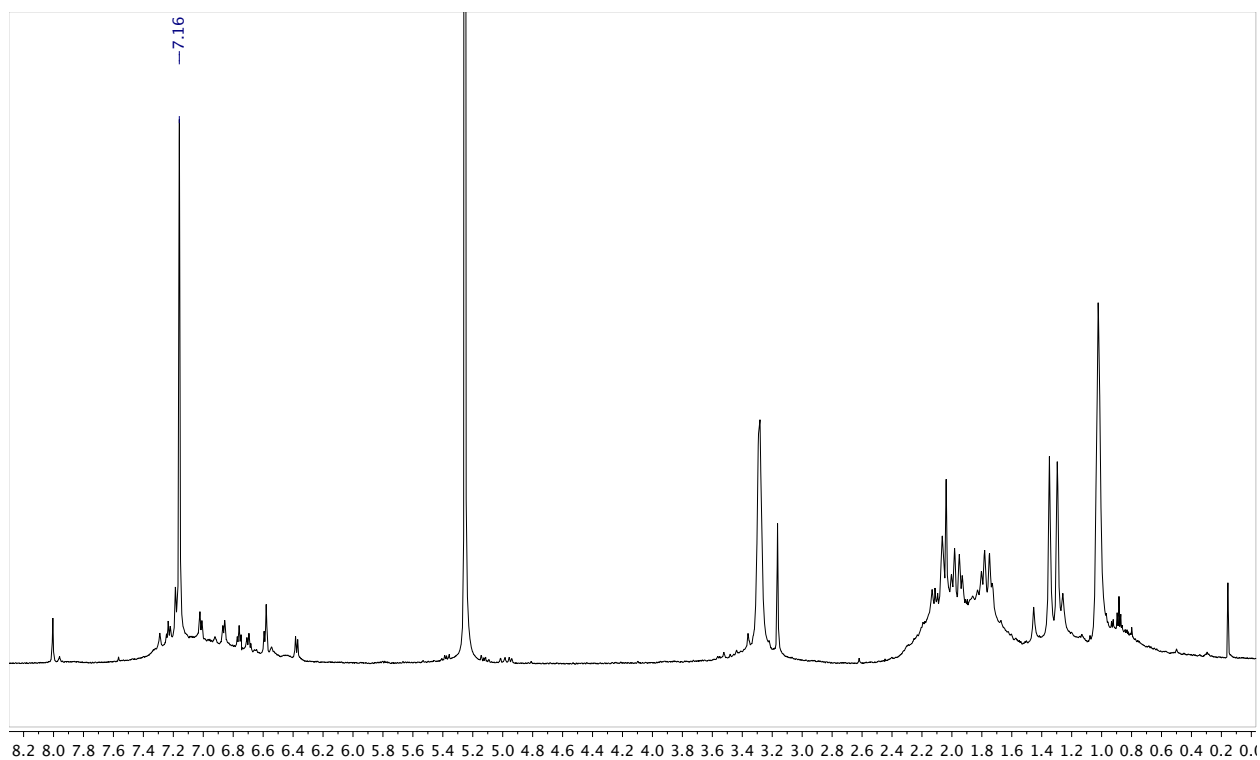


Figure 17. Reaction of (FI)TaMe₄ with B(C₆F₅)₃ under the presence of ethylene. Note the very faint olefinic peaks at δ 5.0 and δ 5.8. Note also that there is no reaction between (FI)TaMe₄ and ethylene alone (see appendix).

Besides their use in the manufacturing of LLDPE, light olefins bear little industrial value. If they can be upgraded to heavier oligomers like C₁₀ or C₁₂ however, they become important precursors for jet fuel and car oil. This motivation prompted the exploration of the higher olefin dimerization capability of (FI)TaMe₂Cl₂ and (FI)TaMe₄. Several neat reactions with both compounds and respective activators along with either 1-hexene or 1-pentene were conducted. Under an excess of diethyl zinc, (FI)TaMe₂Cl₂ shows no evidence of dimerizing 1-pentene or 1-hexene as analyzed by ¹H NMR and gas chromatography. Preliminary results indicate that even under varying equivalents of diethyl zinc to (FI)TaMe₂Cl₂ (0.25:1, 0.50:1, 1:1, 5:1), dimers (C₁₂ alkene isomers) fail to form. Dimerization of 1-hexene also seems unfeasible with (FI)TaMe₄ and one equivalent of B(C₆F₅)₃. Although it is yet to be concluded definitively that these complexes may not dimerize α-olefins, it is interesting that the compounds seem selective towards ethylene dimerization. As mentioned previously (see Tantalum Metalation section), the tantalocyclopentane catalysts reported by Schrock have been shown to selectively dimerize α-olefins and ethylene with a substantially lower rate of dimerization with ethylene. In this case, ethylene forms more stable metallocycles when it inserts, and as such is less prone to ring contraction and generation of 1-butene.¹² However, as no mechanistic studies have been done, it is unclear whether our system undergoes a Cossee or metallacycle mechanism.

Conclusions

Phenoxy Imine (FI) compounds have proved worthy ethylene polymerization catalysts,⁷ and as of recently trimerization catalysts as well.^{6,8} For the purpose of this study, two tantalum phenoxy-imine complexes (FI)TaMe₂Cl₂ and (FI)TaMe₄ have been synthesized and tested for ethylene oligomerization, employing a previously published phenoxy-imine ligand (FI)H.⁶ Both complexes are capable of dimerizing ethylene to 1-butene when activated with B(C₆F₅)₃ ((FI)TaMe₄) along with ZnEt₂ and EtMgCl ((FI)TaMe₂Cl₂). As no mechanistic

studies have been performed, the mechanism of dimerization is unclear and could either be Cossee or metallacycle.

Experimental Methods

General Considerations

Unless otherwise noted, all manipulations of air-sensitive compounds were carried under a nitrogen atmosphere, with standard high-vacuum line and glove box techniques. NMR spectra were recorded on Varian spectrometers at field strengths of 300MHz, 400MHz, and 600MHz in C₆D₆ or CDCl₃ at ambient temperature. Chemical shifts are reported in ppm, and are referenced to residual solvent peaks. All pertinent solvents are purified and degassed by using standard procedures.

*Synthesis of 2-adamantyl-*p*-cresol*

The synthesis of (FI)H was adapted from the literature procedure.⁹ To a 500 mL round bottom flask with a magnetic stir bar was added *p*-cresol (17.04 g, 0.158 mol), CH₂Cl₂ (150 mL), and 1-adamantanol (24.9 g, 0.164 mol) in air at room temperature. The colorless solution was stirred for 10 min. and treated dropwise with conc. H₂SO₄ (9 mL) over a period of 20 minutes, and then stirred for an additional 30 minutes. After this period, ice water (150 mL) was added slowly, and the solution was neutralized with NaOH_(aq) (2 M, *ca.* 160 mL), producing a white slurry. CH₂Cl₂ (200 mL) was added and the organic layer was separated and collected. The aqueous layer was extracted with CH₂Cl₂ (2 × 200 mL), the organic portions were combined and washed with brine (100 mL), and the volatiles were removed by rotary evaporation giving a sticky white solid. The solid was treated with MeOH (200 mL), warmed to a gentle reflux, and then allowed to cool and filtered. The precipitate was extracted with an additional portion of MeOH (200 mL), filtered, and combined with the first MeOH extraction. The volatiles were removed by rotary

evaporation, and the residue dried *in vacuo* giving 2-adamantyl-*p*-cresol as a white solid powder (24.0 g, 63% yield).

Synthesis of 3-adamantyl-2-hydroxy-5-methylbenzaldehyde

The synthesis of (FI)H was adapted from the literature procedure.⁹ To a 500mL round bottom flask with magnetic stir bar was added 2-adamantyl-*p*-cresol (8.0 g, 0.033 mol), hexamethylenetetraamine (9.25 g, 0.068 mol) and glacial acetic acid (100 mL) in air. The mixture was heated at 110 °C while stirring for 5 hrs, with an equipped reflux condenser. After 5 hrs, the solution changed color from clear to orange, and it was allowed to cool to room temperature. To the cooled mixture was added water (ca. 12 mL) dropwise very gradually while stirring, and the solution was allowed to stir overnight. The precipitant was filtered and washed with MeOH (20 mL). To the filtrate was added water (ca. 40 mL) dropwise and the precipitant was filtered once more. The off-white precipitants were then combined, filtered, washed with MeOH (40 mL) for 2 hrs and dried *in vacuo* to give a pale yellow solid (5.6 g, Yield: 63%)

Synthesis of 2-(2-methoxyphenyl)aniline

The synthesis of (FI)H was adapted from the literature procedure.⁹ To a 350 mL ampoule with magnetic stir bar was added 2-methoxyphenylboronic acid (10 g, 0.066 mol), 2-bromoaniline (11.93 g, 0.070 mol), Pd(PPh₃)₄ (2.2 g, 1.90 mmol), K₂CO₃ (20.00 g, 0.145 mol) and toluene (160 mL). The stirred mixture was heated at 115 °C for 22 hours, after which it was cooled to room temperature. To the cooled mixture was added H₂O (100 mL). The dark orange organic layer was then separated, and the aqueous layer was extracted with toluene (50 mL). The organic layers were combined, dried with Na₂SO₄, filtered, and the volatiles removed by rotary evaporation, giving a dark brown oil. The oil was purified by flash column chromatography to give a white crystalline solid (8.5 g, 65% yield).

Synthesis of (FI)H

The synthesis of (FI)H was adapted from the literature procedure.⁹ To a 250 mL round bottom flask equipped with a magnetic stir bar was added 2-(2'-methoxyphenyl)aniline (4.26 g, 0.021 mol), 3-adamantyl-2-hydroxy-5-methylbenzaldehyde (5.50 g, 0.020 mol), EtOH (100 mL), and AcOH (*ca.* 0.2 mL) consecutively in air. The off-white suspension was stirred for 3 days at room temperature, thereby forming a bright yellow suspension. The yellow solid was isolated by filtration, washed with pentane (40 mL), and dried *in vacuo*, giving (FI)H as a yellow solid (6.00 g, 65% yield). (see Appendix Figure A11 for ¹H NMR spectrum)

Synthesis of (FI)TaMe₂Cl₂

To a solution of TaMe₃Cl₂ (150 mg, 0.505 mmol) in toluene (1 mL) was added an orange solution of (FI)H (200 mg, 0.443 mmol) in toluene (2ml) dropwise. After 1 min, an orange precipitate formed. The mother liquor was decanted, and the orange powder was washed with toluene (1 mL) and then pentane (2 × 2mL), and finally dried *in vacuo* to afford orange (FI)TaMe₂Cl₂ (271 mg, Yield: 84%). X-ray quality crystals were obtained from a solution of Et₂O at -35°C (Yield: 84%). The molecular structure of (FI)TaMe₂Cl₂ is shown in Figure 6. Anal. calcd.: C, 54.11%; H, 5.23%; N, 1.91%. Found: C, 54.39%; H, 5.51%; N, 1.72%. (see Appendix FigureA1 for ¹H NMR spectrum and Figure A2 for ¹³C NMR spectrum.)

(¹H NMR, 400MHz): 1.58 (s, 6H, TaMe₂), 1.69 (d, AB pattern, 3H of C(CH₂)₃(CH)₃(CH₂)₃), 1.87 (d, AB pattern, 3H of C(CH₂)₃(CH)₃(CH₂)₃), 2.02 (br s, 3H, Ar-Me), 2.12 (br s, 10H of C(CH₂)₃(CH)₃(CH₂)₃), 3.10 (s, 3H, OMe), 6.34 (d, 1H of Ar), 6.56 (s, 1H of Ar), 6.78 (t, 1H of Ar), 6.93 (m, 2H of Ar), 7.08 (dt, 3H of Ar), 7.34 (m, 1H of Ar), 7.65 (d, 2H of Ar), 8.33 (s, 1H of N=CH).

Synthesis of (FI)TaMe₄

A solution of MeMgBr in Et₂O (173 uL, 3M, 0.519 mmol) was added to a stirring suspension of (FI)TaMe₂Cl₂ (200 mg, 0.274 mmol) in Et₂O cooled to -35° C for 10 min.

After this period, the reaction contents change color to a pale yellow color, and 1, 4-dioxane (0.065 ml, 0.76 mmol) was added, causing precipitate to form. The suspension was then filtered through a medium porosity frit with a 1 cm bed of celite, washed with Et₂O (10 mL). The precipitate/celite was then extracted with room temperature Et₂O (2x mL). The extracts deposited yellow crystals after several days, which were isolated, washed with Et₂O (1 mL) and pentane (2 mL) and dried *in vacuo* to give (FI)TiMe₄ as a yellow crystalline solid (80 mg, 42% yield). X-ray quality crystals were obtained by this manner; the molecular structure is shown in Figure 10. Anal. calcd.: C, 60.78%; H, 6.41%; N, 2.03%. Found: C, 59.07%; H, 5.95%; N, 1.89%. (see Appendix FigureA3 for ¹H NMR spectrum and Figure A4 for ¹³C NMR spectrum.)

(¹H NMR, 600MHz): 1.23 (s, 12H, TaMe₄), 1.76 (d, AB pattern, 3H of C(CH₂)₃(CH)₃(CH₂)₃), 1.91 (d, AB pattern, 3H of C(CH₂)₃(CH)₃(CH₂)₃), 2.10 (br s, 3H, Ar-Me), 2.15 (s, 3H of C(CH₂)₃(CH)₃(CH₂)₃), 2.23 (br s, 7H of C(CH₂)₃(CH)₃(CH₂)₃), 2.80 (s, 3H, OMe), 6.23 (d, 1H of Ar), 6.61 (s, 2H of Ar), 6.79 (t, 1H of Ar), 7.00 (dt, 3H of Ar), 7.19 (d, 2H of Ar), 7.31 (s, 2H of Ar), 8.43 (s, 1H of N=CH).

Reaction between (FI)TaMe₂Cl₂ and Et₂Zn in the presence of ethylene

An orange suspension of (FI)TaMe₂Cl₂ (10 mg, 0.014 mmol) in C₆D₆ (*ca.* 0.6 mL) in an NMR tube equipped with a J. Young valve was treated with ZnEt₂ (13 μ L, 0.126 mmol) at room temperature. The sample was analyzed by ¹H NMR. Note that the compound peaks become indistinguishable upon addition of ZnEt₂ and as such, it is difficult to assess the new compound of interest. (see Figure 15) Note also that there is no reaction between just (FI)TaMe₂Cl₂ and ethylene. (Figure 15)

¹H NMR (300MHz, C₆D₆): -0.55 (br s, Zn alkyl compound), 0.80 (s, 6H, ethane), 5.21 (2, 4H, ethylene).

Reaction between (FI)TaMe₂Cl₂ and EtMgCl in the presence of ethylene

An orange suspension of (FI)TaMe₂Cl₂ (10 mg, 0.014 mmol) in C₆D₆ (ca. 0.6 mL) in an NMR tube equipped with a J. Young valve was treated with EtMgCl (13 μ L, 0.026 mmol) at room temperature. The sample was analyzed by ¹H NMR. Note that the compound peaks become indistinguishable upon addition of EtMgCl and as such, it is difficult to assess the new compound of interest. Note also, that there is no reaction between just (FI)TaMe₂Cl₂ and ethylene. (see Figure 15) In addition, as the EtMgCl was not entirely dry, there is an abundance of THF in the spectrum (see Appendix Figure A6).

¹H NMR (300MHz, C₆D₆): -0.69 (br s, Zn alkyl compound), 0.16 (s, 4H, CH₄), 0.80 (s, 6H, ethane), 1.38 (s, 4H, THF), 3.61 (s, 4H, THF), 4.99 (dd, 2H, 1-butene vinylic protons), 5.26 (s, 4H, ethylene), 5.75 (dt, 1H 1-butene vinylic proton).

Reaction between (FI)TaMe₂Cl₂ and dimethyl anilinium

tetrakis(pentafluorophenyl)borate in the presence of ethylene

An orange suspension of (FI)TaMe₂Cl₂ (9.6 mg, 0.013 mmol) in C₆D₆ (ca. 0.6 mL) in an NMR tube equipped with a J. Young valve was treated with dimethylanilinium tetrakis(pentafluorophenyl)borate (9.7 mg, 0.012 mmol) at room temperature presumably to generate [(FI)TaMeCl₂]⁺[B(C₆F₅)₄]⁻ but no such species was observed by ¹H NMR (see Appendix Figure A7). Note that there is no reaction between just (FI)TaMe₂Cl₂ and ethylene. (see Figure 15)

(¹H NMR, 300MHz): 0.16 (s, 4H, CH₄) 1.54 (s, 6H, TaMe₂), 1.70 (d, AB pattern, 3H of C(CH₂)₃(CH)₃(CH₂)₃), 1.86 (d, AB pattern, 3H of C(CH₂)₃(CH)₃(CH₂)₃), 1.90 (s, 6H, methyl groups of dimethyl anilinium), 2.03 (br s, 3H, Ar-Me), 2.11 (br s, 10H of C(CH₂)₃(CH)₃(CH₂)₃), 3.09 (s, 3H, OMe), 5.26 (s, 4H, C₂H₄), 5.66 (s, 1H, N-H⁺), 6.33 (d, 3H, Ar + (CH₃)NH⁺(C₆H₅)), 6.58 (s, 1H of Ar), 6.77 (t, 1H of Ar), 6.90 (m, 4H of Ar + (CH₃)NH⁺(C₆H₅)), 7.08 (dt, 3H of Ar + (CH₃)NH⁺(C₆H₅)), 7.31 (m, 1H of Ar), 7.60 (m, 1H of Ar), 8.33 (s, 1H of N=CH).

Reaction between (FI)TaMe₂Cl₂ and trityl tetrakis(pentafluorophenyl)borate in the presence of ethylene.

An orange suspension of (FI)TaMe₂Cl₂ (10.3 mg, 0.014 mmol) in C₆D₆ (*ca.* 0.6 mL) in an NMR tube equipped with a J. Young valve was treated with trityl tetrakis(pentafluorophenyl)borate (15.3 mg, 0.017 mmol) at room temperature presumably to generate [(FI)TiMeCl₂]⁺[B(C₆F₅)₄]⁻ and MeC(C₆H₅)₃, but it is difficult to tell if this is the observed product by ¹H NMR (see Appendix Figure A8). Many aryl-H, aryl-Me and aryl-admantyl peaks are fairly obscured, and thus only definite peaks are reported.

(¹H NMR, 300MHz): 0.16 (s, 4H, CH₄), 1.55 (s, 6H, TaMe₂), 3.05 (s, 3H, OMe), 5.26 (s, 4H, C₂H₄), 8.24 (s, 1H of N=CH).

Reaction between (FI)TaMe₄ and B(C₆F₅)₃ in the presence of ethylene.

A yellow solution of (FI)TiMe₄ (5 mg, 0.007 mmol) in C₆D₆ (*ca.* 0.6 mL) in an NMR tube equipped with a J. Young valve was treated with B(C₆F₅)₃ (3.7 mg, 0.007 mmol) at room temperature. The sample was analyzed by ¹H NMR demonstrating what is believed to a conversion to [(FI)TiMe₃][MeB(C₆F₅)₃] (*ca.* 100% by ¹H NMR integration). Note that the Ar-adamantyl and Ar-Me peaks are difficult to distinguish. Note also that there is no reaction between (FI)TaMe₄ and ethylene (see Appendix Figure A9).

¹H NMR (600MHz, C₆D₆): 1.02 (br s, 3H of MeB(C₆F₅)₃), 1.30 (s, 3H of TiMe₄), 1.35 (s, 3H of TiMe₄), 1.45 (s, 3H of TiMe₄), 3.17 (s, 3H of OMe), 6.38 (d, 1H of Ar), 6.58 (s, 1H of Ar), 6.73 (m, 3H of Ar), 6.85 (m, 1H of Ar), 7.01 (m, 2H of Ar), 7.17-7.30 (shoulder peaks under solvent peak, 3H of Ar), 8.00 (s, 1H of N=CH).

Reaction between (FI)TaMe₄ and Dimethyl anilinium tetrakis(pentafluorophenyl)borate

A yellow solution of (FI)TiMe₄ (6.5 mg, 0.009 mmol) in C₆D₆ (*ca.* 0.6 mL) in an NMR tube equipped with a J. Young valve was treated with dimethyl anilinium tetrakis(pentafluorophenyl)borate (6.8 mg, 0.008 mmol) at room temperature. The sample

was analyzed by ^1H NMR demonstrating what is believed to a conversion to $[(\text{FI})\text{TiMe}_3]^+[\text{B}(\text{C}_6\text{F}_5)_4]^-$ (see Appendix Figure A10).

(*ca.* 100% by ^1H NMR integration). Note that the Ar-adamantyl, Ar-Me, and dimethylaniline peaks are difficult to distinguish.

^1H NMR (300MHz, C_6D_6): 0.16 (s, 4H, CH_4) 1.33 (br s, 9H, TaMe_3^+), 1.30 (s, 3H of TiMe_4), 2.11 (s, 6H, $(\text{CH}_3)\text{N}(\text{C}_6\text{H}_5)$) 3.14 (s, 3H of OMe), 6.38 (d, 3H, Ar + $(\text{CH}_3)\text{N}(\text{C}_6\text{H}_5)$), 6.50 (s, 1H of Ar), 6.69 (m, 2H of Ar), 6.85 (m, 5H, Ar + $(\text{CH}_3)\text{N}(\text{C}_6\text{H}_5)$), 7.06 (m, 5H of Ar + $(\text{CH}_3)\text{N}(\text{C}_6\text{H}_5)$), 7.97 (s, 1H of $\text{N}=\text{CH}$).

Appendix

Characterization of (FI)TaMe₂Cl₂ and (FI)TaMe₄.

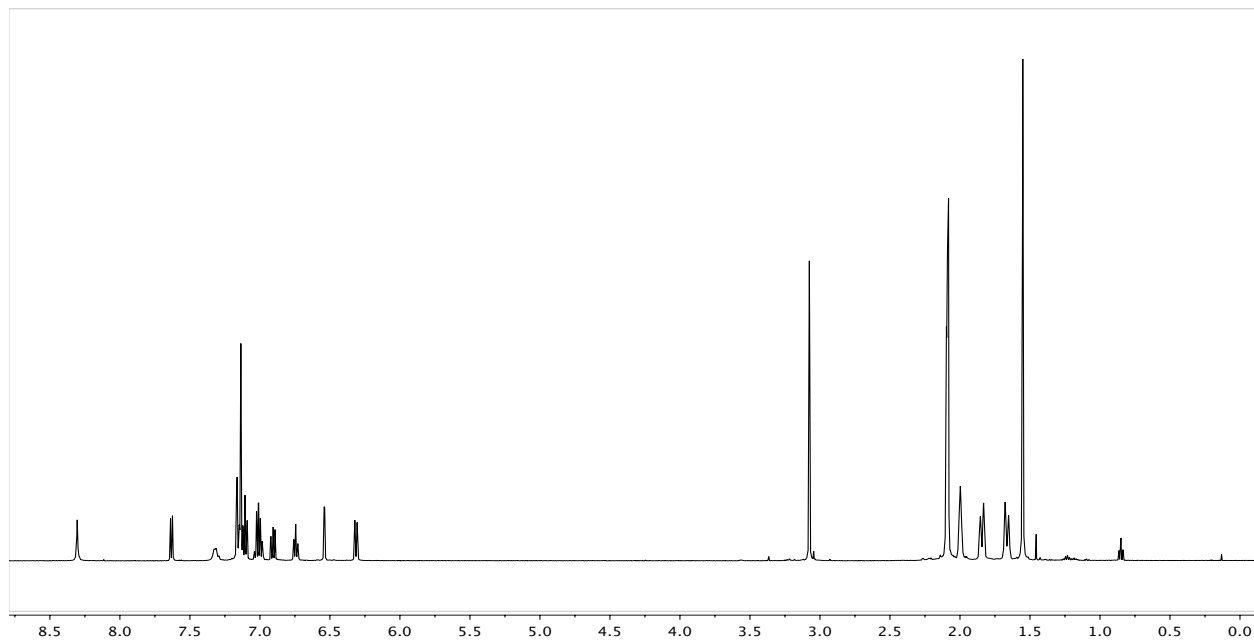


Figure A1. ¹H NMR spectrum of (FI)TaMe₂Cl₂ in C₆D₆ at 25°C.

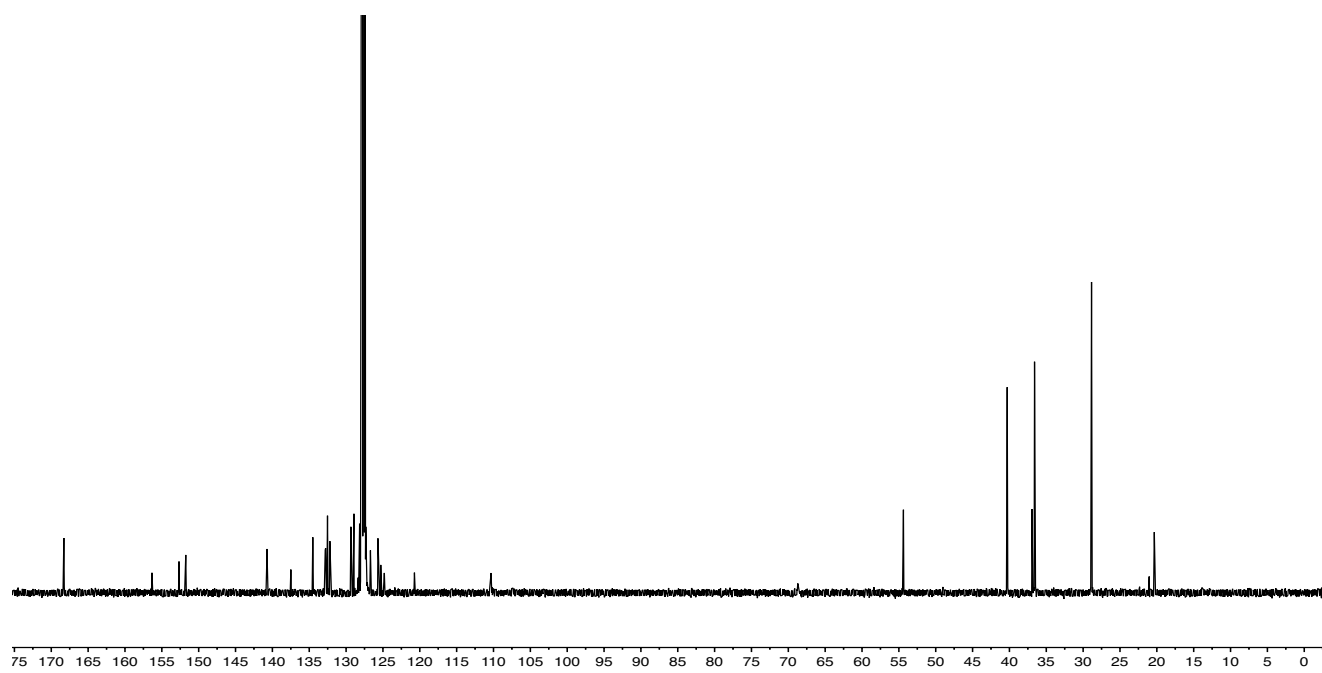


Figure A2. ¹³C{¹H} NMR spectrum of (FI)TaMe₂Cl₂ in C₆D₆ at 25°C.

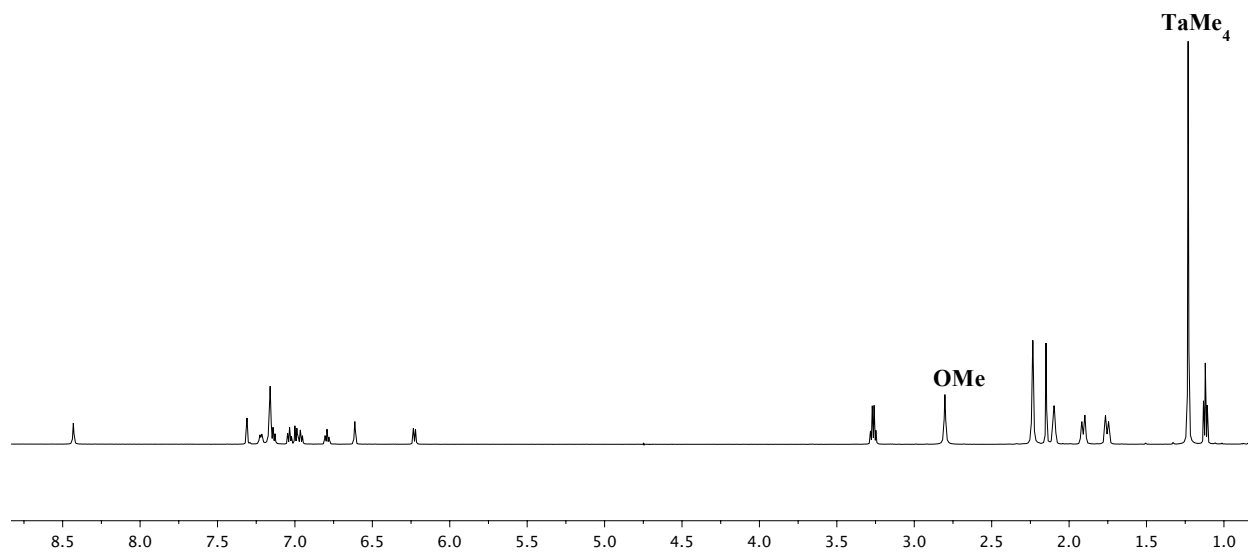


Figure A3. ^1H NMR spectrum of $(\text{FI})\text{TaMe}_4$ in C_6D_6 at 25°C .

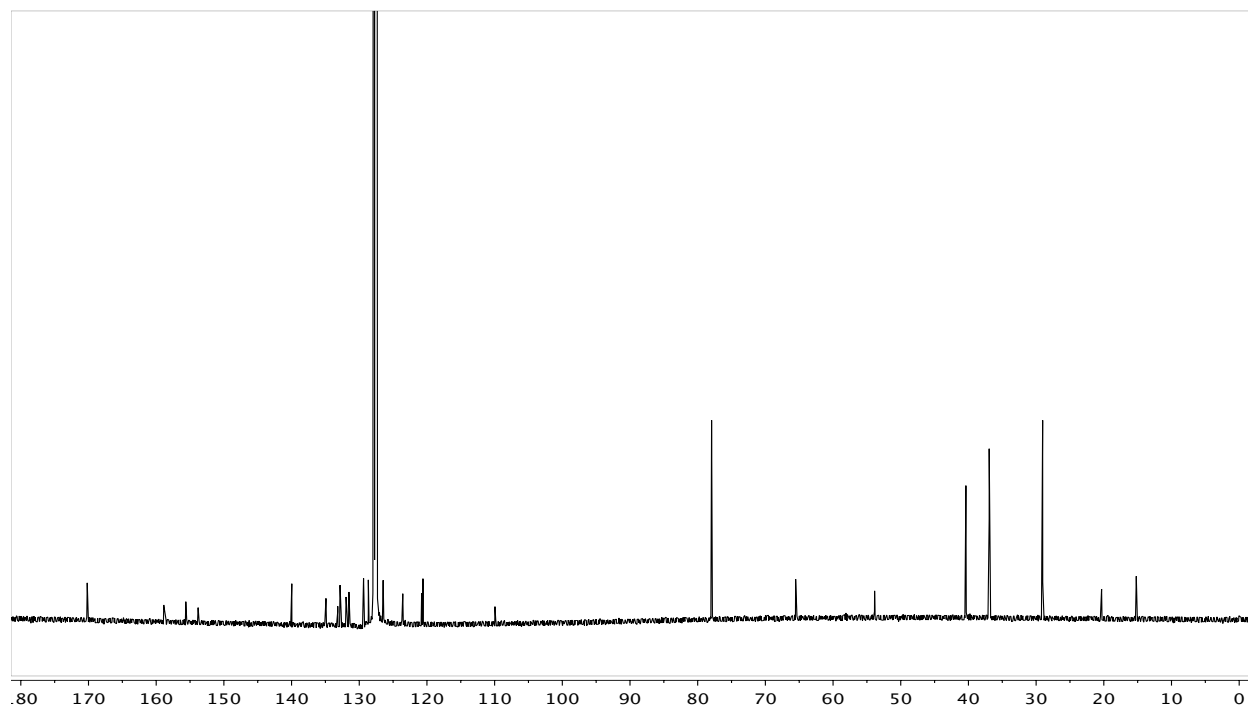


Figure A4. $^{13}\text{C}\{^1\text{H}\}$ NMR spectrum of $(\text{FI})\text{TaMe}_4$ in C_6D_6 at 25°C .

Reactions of (FI)TaMe₂Cl₂ and (FI)TaMe₄ with various activators and ethylene.

See Figure 15 for Reaction of (FI)TaMe₂Cl₂ with ethylene.

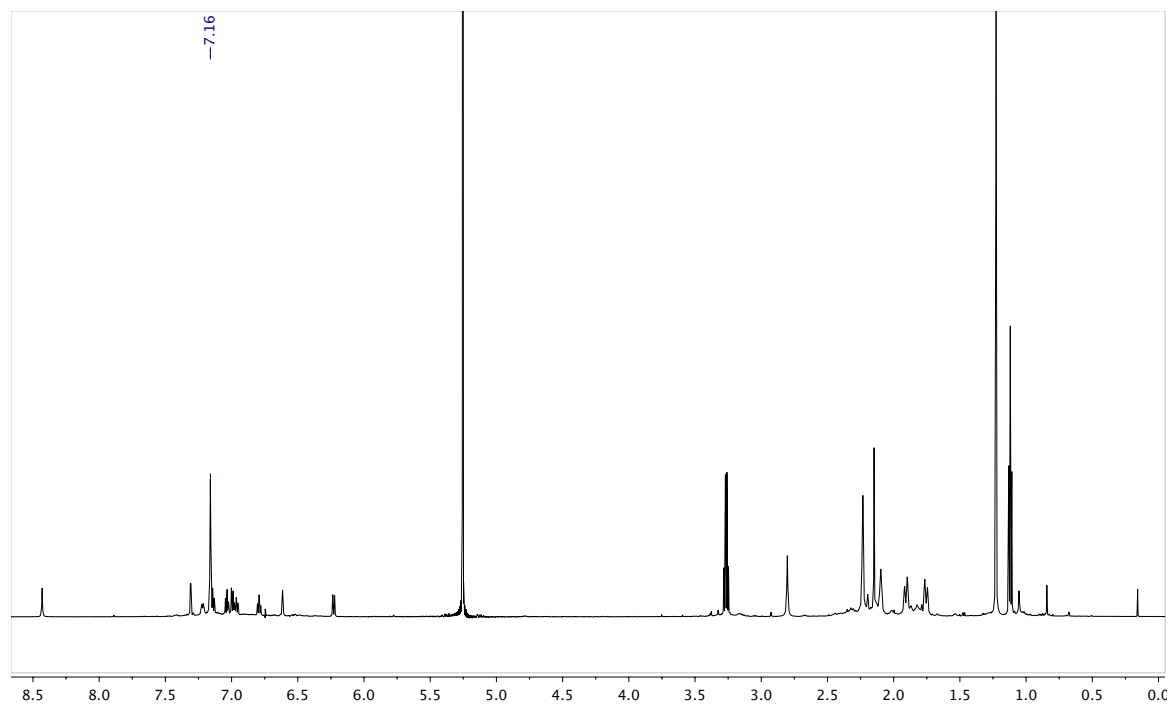


Figure A5. Reaction of (FI)TaMe₂Cl₂ with ethylene. Compounds peaks remain unchanged and a peak at δ 5.25 denotes ethylene.

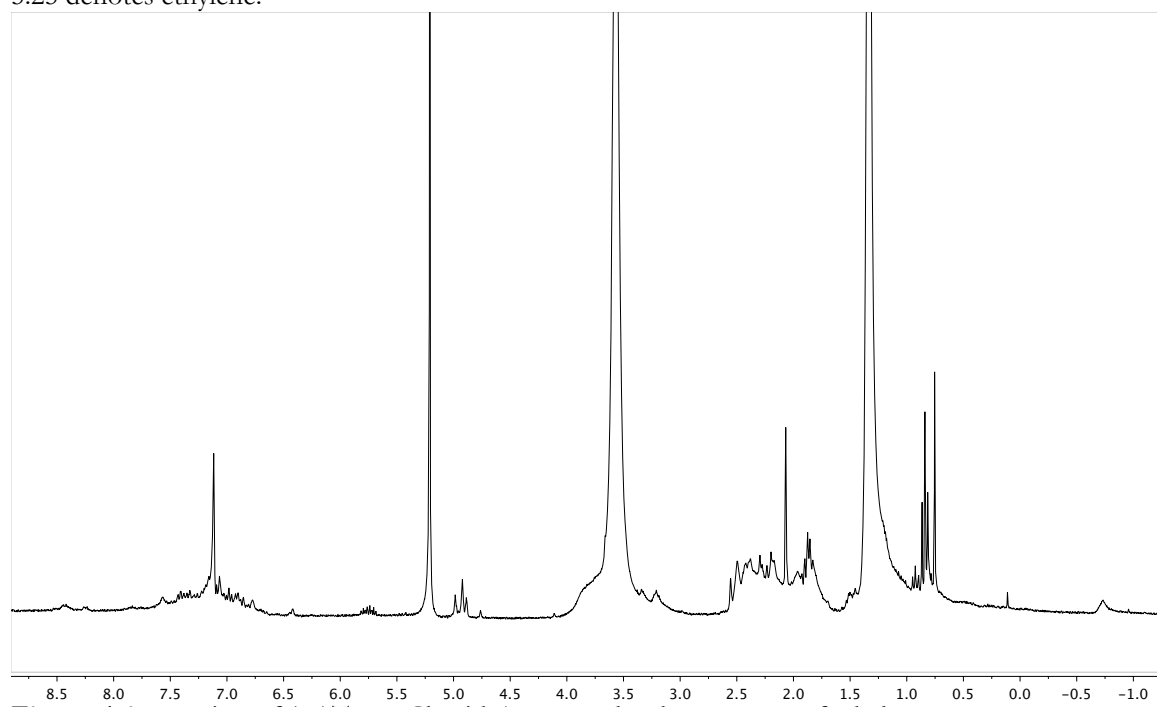


Figure A6. Reaction of (FI)TaMe₂Cl₂ with ZnEt₂ under the presence of ethylene.

See Figure 15 for reaction of $(FI)TaMe_2Cl_2$ with $ZnEt_2$ under the presence of ethylene.

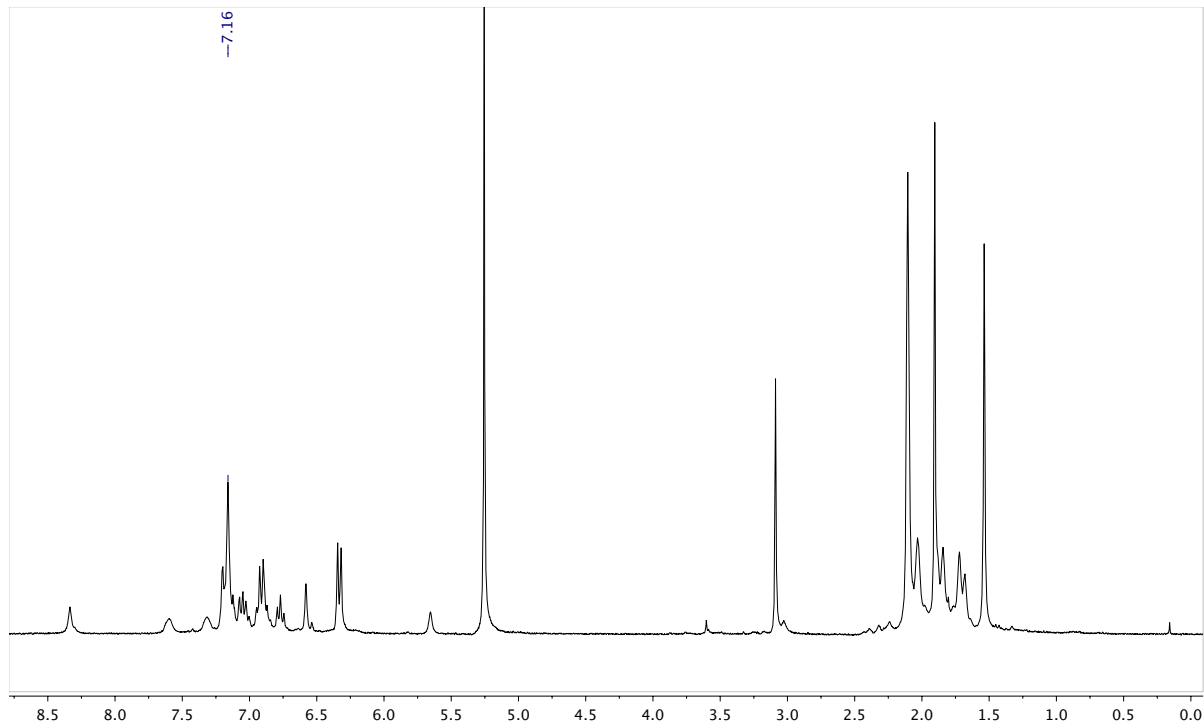


Figure A7. Reaction of $(FI)TaMe_2Cl_2$ with dimethylanilinium tetrakis(pentafluorophenyl)borate under the presence of ethylene.

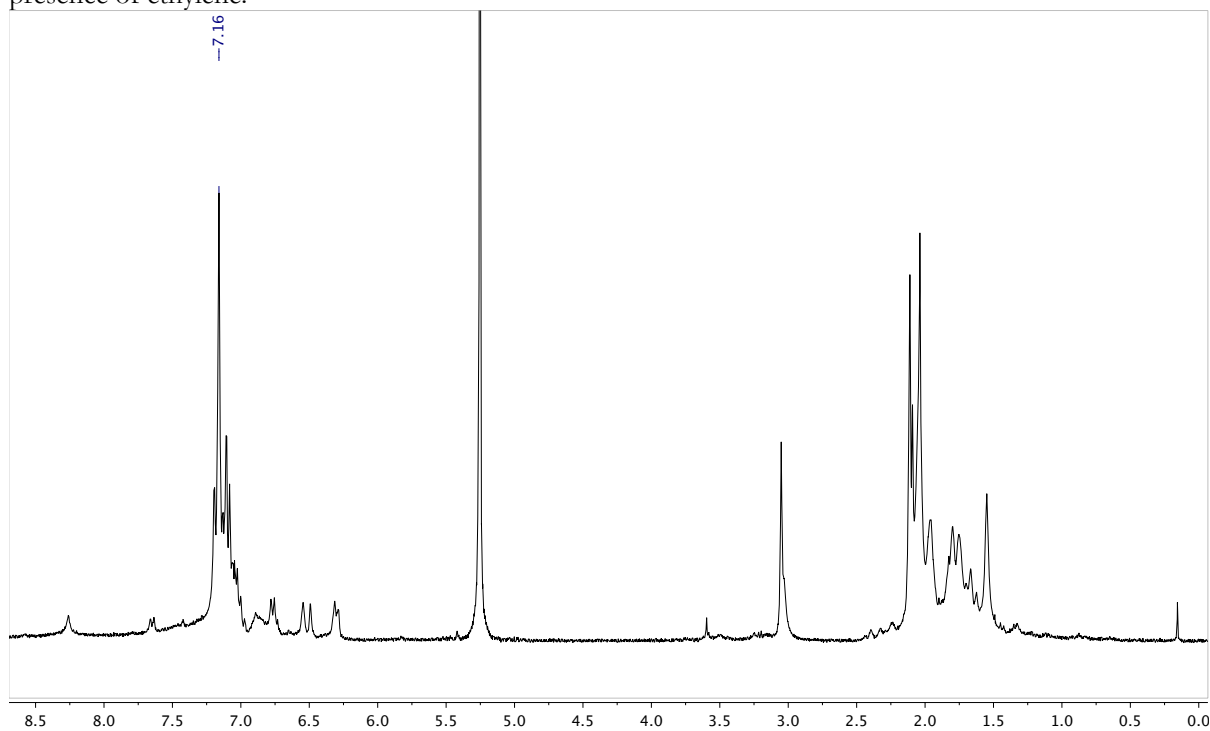


Figure A8. Reaction of $(FI)TaMe_2Cl_2$ with trityl tetrakis(pentafluorophenyl)borate under the presence of ethylene.

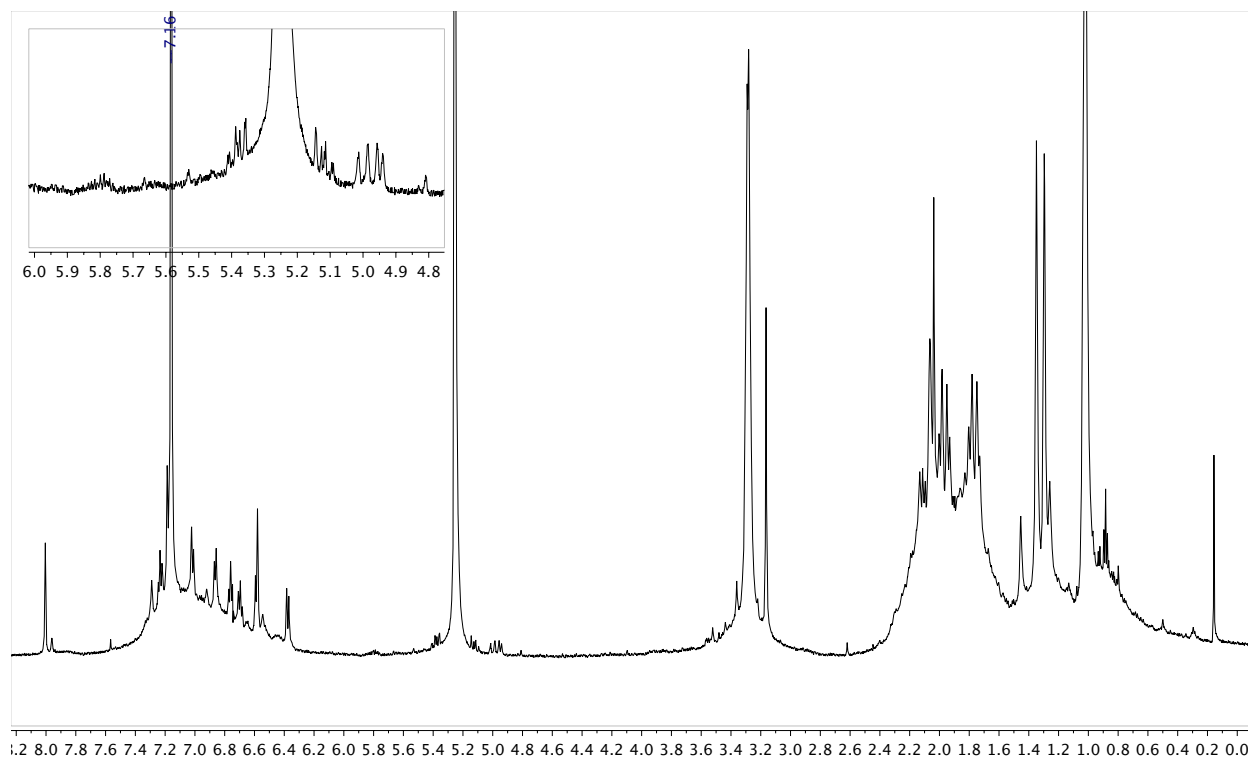


Figure A9. Reaction of (FI)TaMe₄ with tris(pentafluorophenyl)borate under the presence of ethylene.

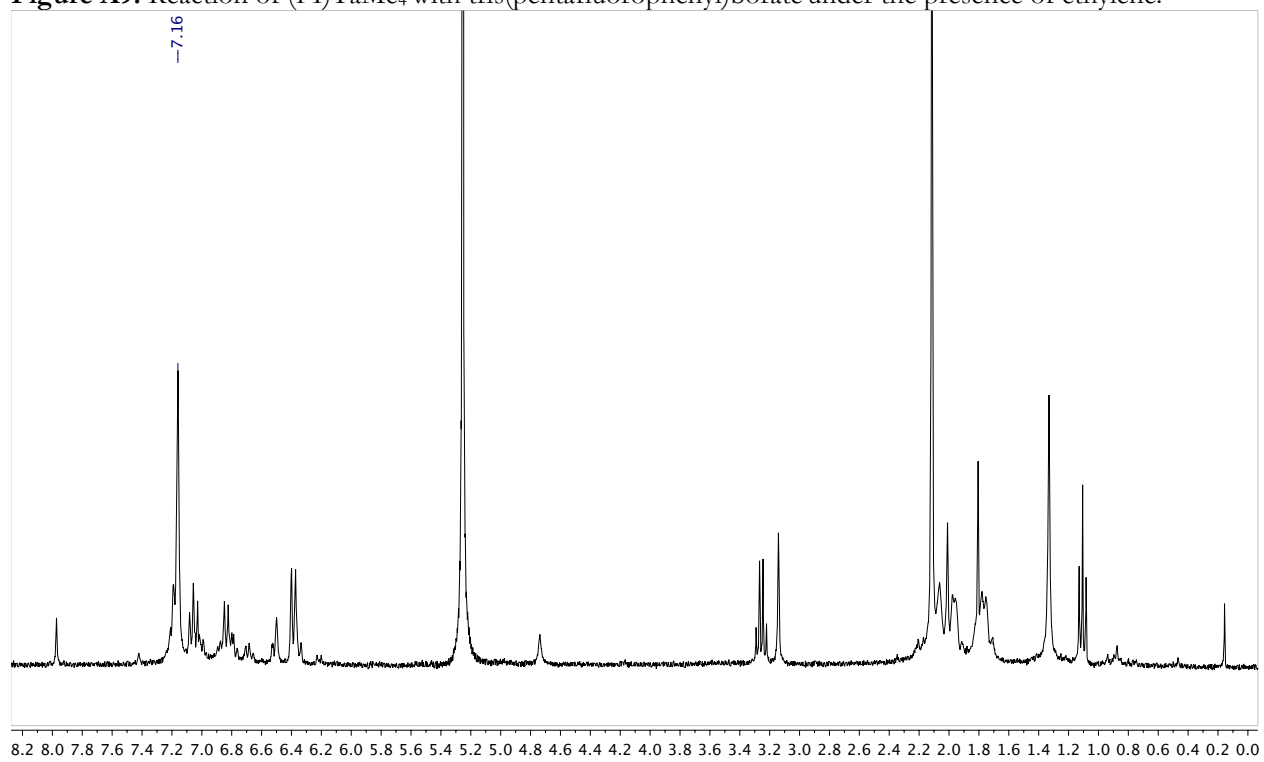


Figure A10. Reaction of (FI)TaMe₄ with dimethylanilinium tetrakis(pentafluorophenyl)borate under the presence of ethylene.

Characterization of (FI)H/Zr reactions

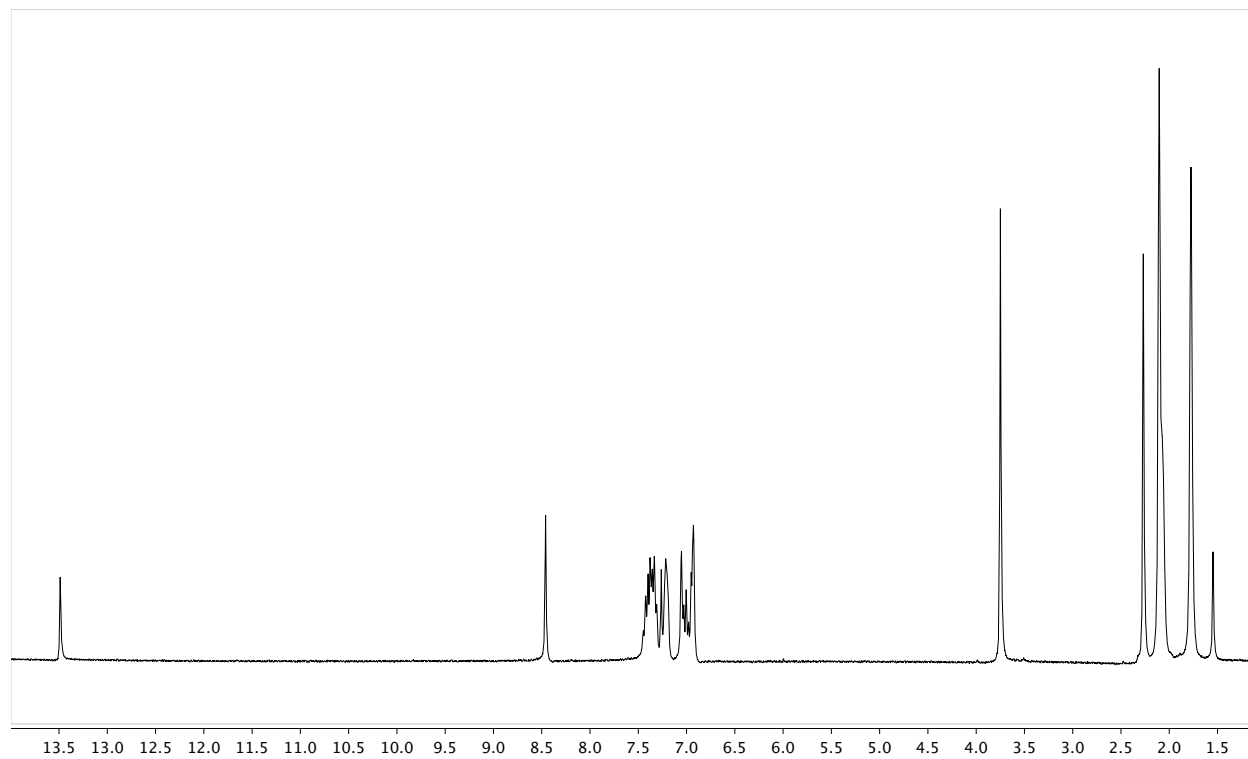


Figure A11. ¹H NMR spectrum of (FI)H in CDCl₃ at 25°C.

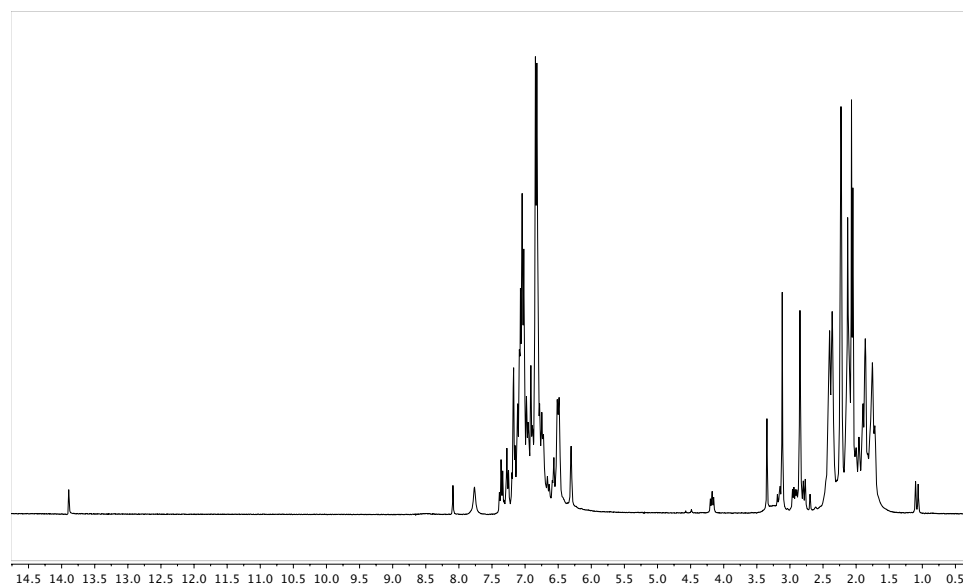


Figure A12. ¹H NMR spectrum of reaction of (FI)H and ZrBn₄. The nature of the generated compounds is unclear.

Table A1. Crystal, intensity collection and refinement data.

	(FI)TaMe₂Cl₂	(FI)TaMe₄	(FI)Zr(THF)Cl₄
lattice	Monoclinic	Monoclinic	Monoclinic
formula	C ₃₃ H ₃₈ Cl ₂ NO ₂ Ta	C ₄₀ H ₄₀ NO ₂ Ta	C ₄₀ H ₄₀ Cl ₄ NO ₂ Zr
formula weight	723.49	747.68	799.75
space group	<i>P2₁/n</i>	<i>P2₁/c</i>	<i>P2₁/n</i>
<i>a</i> /Å	14.6701(7)	11.1194(14)	9.7573(8)
<i>b</i> /Å	13.7321(6)	18.748(3)	15.1510(12)
<i>c</i> /Å	14.8844(7)	17.545(2)	26.837(2)
α /°	90.00	90.00	90.00
β /°	92.702(3)	107.410(7)	92.852(5)
γ /°	90.00	90.00	90.00
<i>V</i> /Å ³	2995.1(2)	3490.1(8)	3962.5(6)
<i>Z</i>	4	4	4
temperature (K)	100	296(2)	296(2)
radiation (λ , Å)	0.71073	0.71073	0.71073
ρ (calcd.), g cm ⁻³	1.624	1.423	1.341
μ (Mo K α), mm ⁻¹	3.88	3.183	0.581
θ max, deg.	34.91	37.80	33.25
no. of data collected	99385	193194	134731
no. of data	12358	18666	16549
no. of parameters	356	401	461
<i>R</i> ₁ [<i>I</i> > 2 σ (<i>I</i>)]	0.0264	0.0365	0.0614
<i>wR</i> ₂ [<i>I</i> > 2 σ (<i>I</i>)]	0.0507	0.1287	0.1872
<i>R</i> ₁ [all data]	0.0428	0.0528	0.1004
<i>wR</i> ₂ [all data]	0.0549	0.1463	0.2085
GOF	1.035	1.115	1.324

References:

- (1) McGuinness, D. S. *Chem. Rev.* **2011**, *111*, 2321.
- (2) Agapie, T. *Coord. Chem. Rev.* **2011**, *255*, 861.
- (3) Hagen, H. *Ind. Eng. Chem.* **2006**, *45*, 3544.
- (4) Belov, G. P.; Dzhabiev, T. S.; Kolesnikov, I. M. *J. Mol. Catal.* **1980**, *14*, 105.
- (5) Agapie, T.; Schofer, S. J.; Labinger, J. A.; Bercaw, J. E. *J. Am. Chem. Soc.* **2003**, *126*, 1304.
- (6) Suzuki, Y.; Kinoshita, S.; Shibahara, A.; Ishii, S.; Kawamura, K.; Inoue, Y.; Fujita, T. *Organometallics* **2010**, *29*, 2394.
- (7) Makio, H.; Terao, H.; Iwashita, A.; Fujita, T. *Chem. Rev.* **2011**, *111*, 2363.
- (8) Song, K.-M.; Gao, H.-Y.; Liu, F.-S.; Pan, J.; Guo, L.-H.; Zai, S.-B.; Wu, Q. *Catal. Letter.* **2009**, *131*, 566.
- (9) Sattler, A.; Labinger, J. A.; Bercaw, J. E. *J. Am. Chem. Soc.* **2013**, *32*, 6899.
- (10) Deckers, P. J. W.; Hessen, B.; Teuben, J. H. *Organometallics* **2002**, *21*, 5122.
- (11) Tobisch, S.; Ziegler, T. *J. Am. Chem. Soc.* **2004**, *126*, 9059.
- (12) McLain, S. J.; Sancho, J.; Schrock, R. R. *J. Am. Chem. Soc.* **1979**, *102*, 5610.
- (13) Andes, C.; Harkins, S. B.; Murtuza, S.; Oyler, K.; Sen, A. *J. Am. Chem. Soc.* **2001**, *123*, 7423.
- (14) Arteaga-Muller, R.; Tsurugi, H.; Saito, T.; Yanagawa, M.; Oda, S.; Mashima, K. *J. Am. Chem. Soc.* **2009**, *131*, 5370.
- (15) Juvinal, G. L. *J. Am. Chem. Soc.* **1964**, *86*, 4202.
- (16) (a) Hall, M. B.; Fenske, R. F. *Inorg. Chem.* **1972**, *11*, 768.
(b) Bursten, B. E.; Jensen, J. R.; Fenske, R. F. *J. Chem. Phys.* **1978**, *68*, 3320.
(c) Manson, J.; Webster, C. E.; Perez, L. M.; Hall, M. B.
<http://www.chem.tamu.edu/jimp2/index.html>.
- (17) Version 2.0, June 1993; Lichtenberger, D. L. Department of Chemistry, University of Arizona, Tucson, AZ 85721.

- (18) Bazan, G. C.; Rodriguez, G. *Polyhedron* **1995**, *14*, 93.
- (19) Horrillo-Martinez, P.; Patrick, B. O.; Schafer, L. L.; Fryzuk, M. D. *Dalton Trans.* **2012**, *41*, 1609.
- (20) Kleinhenz, S.; Pfenning, V.; Seppelt, K. *Chem. Eur. J.* **1998**, *4*, 1687.
- (21) Roessler, B.; Kleinhenz, S.; Seppelt, K. *Chem. Comm.* **2000**, 1039.